

LHC final states and their potential experimental and theoretical accuracies

Amanda Cooper-Sarkar, Michael Dittmar, Günther Dissertori, Claire Gwenlan, Hasko Stenzel, Alessandro Tricoli

1 LHC final states and their potential experimental and theoretical accuracies ¹

1.1 Introduction

Cross section calculations and experimental simulations for many LHC reactions, within the Standard Model and for many new physics scenarios have been performed during the last 20 years. These studies demonstrate how various final states might eventually be selected above Standard Model backgrounds and indicate the potential statistical significance of such measurements. In general, these studies assumed that the uncertainties from various sources, like the PDF uncertainties, the experimental uncertainties and the various signal and background Monte Carlo simulations will eventually be controlled with uncertainties small compared to the expected statistical significance. This is the obvious approach for many so called discovery channels with clean and easy signatures and relatively small cross sections.

However, during the last years many new and more complicated signatures, which require more sophisticated selection criteria, have been discussed. These studies indicate the possibility to perform more ambitious searches for new physics and for precise Standard Model tests, which would increase the physics potential of the LHC experiments. Most of these studies concentrate on the statistical significance only and potential systematic limitations are rarely discussed.

In order to close this gap from previous LHC studies, questions related to the systematic limits of cross section measurements from PDF uncertainties, from imperfect Standard Model Monte Carlo simulations, from various QCD uncertainties and from the efficiency and luminosity uncertainties were discussed within the PDF working group of this first HERA-LHC workshop. The goal of the studies presented during the subgroup meetings during the 2004/5 HERA LHC workshop provide some answers to questions related to these systematic limitations. In particular, we have discussed potential experimental and theoretical uncertainties for various Standard Model signal cross sections at the LHC. Some results on the experimental systematics, on experimental and theoretical uncertainties for the inclusive W, Z and for diboson production, especially related to uncertainties from PDF's and from higher order QCD calculations are described in the following sections.

While it was not possible to investigate the consequences for various aspects of the LHC physics potential in detail, it is important to keep in mind that many of these Standard Model reactions are also important backgrounds in the search for the Higgs and other exotic phenomena. Obviously, the consequences from these unavoidable systematic uncertainties need to be investigated in more detail during the coming years.

1.2 Measuring and interpreting cross sections at the LHC ²

The LHC is often called a machine to make discoveries. However, after many years of detailed LHC simulations, it seems clear that relatively few signatures exist, which do not involve cross section measurements for signals and the various backgrounds. Thus, one expects that cross section measurements for a large variety of well defined reactions and their interpretation within or perhaps beyond the Standard Model will be one of the main task of the LHC physics program.

While it is relatively easy to estimate the statistical precision of a particular measurement as a function of the luminosity, estimates of potential systematic errors are much more complicated. Furthermore,

¹Subsection coordinator: Michael Dittmar

²Contributing author: Michael Dittmar

as almost nobody wants to know about systematic limitations of future experiments, detailed studies are not rewarding. Nevertheless, realistic estimates of such systematic errors are relevant, as they might allow the LHC community to concentrate their efforts on the areas where current systematic errors, like the ones which are related to uncertainties from Parton Distribution Functions (PDF) or the ones from missing higher order QCD calculations, can still be improved during the next years.

In order to address the question of systematics, it is useful to start with the basics of cross section measurements. Using some clever criteria a particular signature is separated from the data sample and the surviving N_{observed} events can be counted. Backgrounds, $N_{\text{background}}$, from various sources have to be estimated either using the data or some Monte Carlo estimates. The number of signal events, N_{signal} , is then obtained from the difference. In order to turn this experimental number of signal events into a measurement one has to apply a correction for the efficiency. This experimental number can now be compared with the product of the theoretical production cross section for the considered process and the corresponding Luminosity. For a measurement at a hadron collider, like the LHC, processes are calculated on the basis of quark and gluon luminosities which are obtained from the proton-proton luminosity “folded” with the PDF’s.

In order to estimate potential systematic errors one needs to examine carefully the various ingredients to the cross section measurement and their interpretation. First, a measurement can only be as good as the impact from of the background uncertainties, which depend on the optimized signal to background ratio. Next, the experimental efficiency uncertainty depends on many subdetectors and their actual real time performance. While this can only be known exactly from real data, one can use the systematic error estimates from previous experiments in order to guess the size of similar error sources for the future LHC experiments. We are furthermore confronted with uncertainties from the PDF’s and from the proton-proton luminosity. If one considers all these areas as essentially experimental, then one should assign uncertainties originating from imperfect knowledge of signal and background cross sections as theoretical.

Before we try to estimate the various systematic errors in the following subsections, we believe that it is important to keep in mind that particular studies need not to be much more detailed than the largest and limiting uncertainty, coming from either the experimental or the theoretical area. Thus, one should not waste too much time, in order to achieve the smallest possible uncertainty in one particular area. Instead, one should try first to reduce the most important error sources and if one accepts the “work division” between experimental and theoretical contributions, then one should simply try to be just a little more accurate than either the theoretical or the experimental colleagues.

1.2.1 Guessing experimental systematics for ATLAS and CMS

In order to guess experimental uncertainties, without doing lengthy and detailed Monte Carlo studies, it seems useful to start with some simple and optimistic assumptions about ATLAS and CMS³.

First of all, one should assume that both experiments can actually operate as planned in their proposals. As the expected performance goals are rather similar for both detectors the following list of measurement capabilities looks as a reasonable first guess.

- Isolated electrons, muons and photons with a transverse momentum above 20 GeV and a pseudorapidity η with $|\eta| \leq 2.5$ are measured with excellent accuracy and high (perhaps as large as 95% for some reactions) “homogeneous” efficiency. Within the pseudo rapidity coverage one can assume that experimentalists will perhaps be able, using the large statistics from leptonic W and Z decays, to control the efficiency for electrons and muons with a 1% accuracy. For simplicity, one can also assume that these events will allow to control measurements with high energy photons to

³Up to date performance of the ATLAS and CMS detectors and further detailed references can be found on the corresponding homepages <http://atlas.web.cern.ch/Atlas/> and <http://cmsinfo.cern.ch/welcome.html/>

a similar accuracy. For theoretical studies one might thus assume that high p_t electrons, muons and photons and $|\eta| \leq 2.5$ are measured with a systematic uncertainty of $\pm 1\%$ for each lepton (photon).

- Jets are much more difficult to measure. Optimistically one could assume that jets can be seen with good efficiency and angular accuracy if the jet transverse momentum is larger than 30 GeV and if their pseudo rapidity fulfills $|\eta| \leq 4.5$. The jet energy resolution is not easy to quantify, but numbers could be given using some “reasonable” assumptions like $\Delta E/E \approx 100 - 150\%/\sqrt{E}$. For various measurements one want to know the uncertainty of the absolute jet energy scale. Various tools, like the decays of $W \rightarrow q\bar{q}$ in $t\bar{t}$ events or the photon-jet final state, might be used to calibrate either the mean value or the maximum to reasonably good accuracy. We believe that only detailed studies of the particular signature will allow a quantitative estimate of the uncertainties related to the jet energy scale measurements.
- The tagging of b-flavoured jets can be done, but the efficiency depends strongly on the potential backgrounds. Systematic efficiency uncertainties for the b-tagging are difficult to quantify but it seems that, in the absence of a new method, relative b-tagging uncertainties below $\pm 5\%$ are almost impossible to achieve.

With this baseline LHC detector capabilities, it seems useful to divide the various high q^2 LHC reactions into essentially five different non overlapping categories. Such a division can be used to make some reasonable accurate estimates of the different systematics.

- Drell–Yan type lepton pair final states. This includes on– and off–shell W and Z decays.
- γ -jet and $\gamma\gamma X$ final states.
- Diboson events of the type WW , WZ , ZZ , $W\gamma$ with leptonic decays of the W and Z bosons. One might consider to include the Standard Model Higgs signatures into this group of signatures.
- Events with top quarks in the final state, identified with at least one isolated lepton.
- Hadronic final states with up to $n(=2,3 \dots)$ Jets and different p_t and mass.

With this “grouping” of experimental final states, one can now start to analyze the different potential error sources. Where possible, one can try to define and use relative measurements of various reactions such that some systematic errors will simply cancel.

Starting with the resonant W and Z production with leptonic decays, several million of clean events will be collected quickly, resulting in relative statistical errors well below $\pm 1\%$. Theoretical calculations for these reactions are well advanced and these reactions are among the best understood LHC final states allowing to build the most accurate LHC Monte Carlo generators. Furthermore, some of the experimental uncertainties can be reduced considerably if ratio measurements of cross section, such as W^+/W^- and Z/W , are performed. The similarities in the production mechanism should also allow to reduce theoretical uncertainties for such ratios. The experimental counting accuracy of W and Z events, which includes background and efficiency corrections, might achieve eventually uncertainties of 1% or slightly better for cross section ratios.

Furthermore, it seems that the shape of the p_t distribution of the Z, using the decay into electron pairs ($pp \rightarrow ZX \rightarrow e+e^-X$), can be determined with relative accuracies of much less than 1%. This distribution, shown in figure 1, can be used to tune the Monte Carlo description of this particular process. This tuning of the Monte Carlo can than be used almost directly to predict theoretically also the W p_t spectrum, and the p_t spectrum for high mass Drell-Yan lepton pair events. Once an accurate model description of these Standard Model reactions is achieved one might use these insights also to predict the p_t spectrum of other well defined final states.

From all the various high q^2 reactions, the inclusive production of W and Z events is known to be the theoretically best understood and best experimentally measurable LHC reaction. Consequently, the

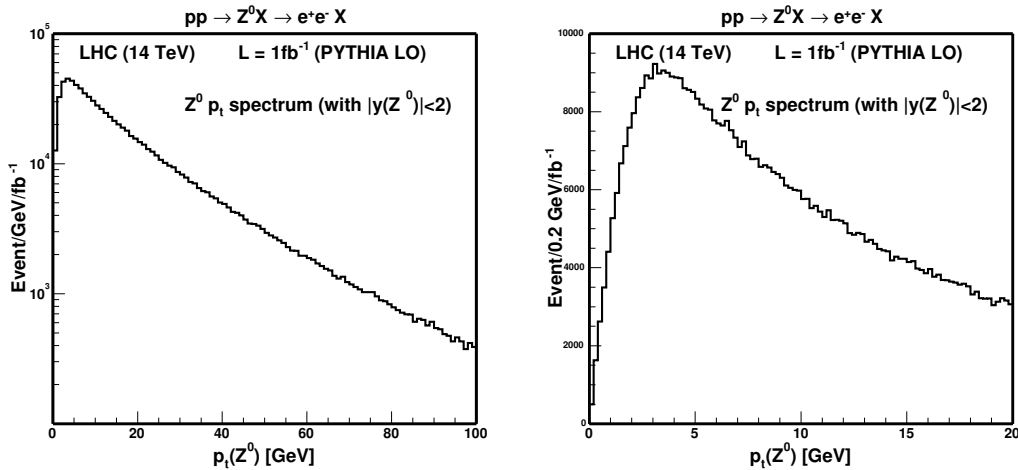


Fig. 1: Simple simulation of a potential measurement of the $Z p_t$ spectrum, possible with a luminosity of only 1 fb^{-1} . Who will be able to predict this p_t spectrum in all its beauty and with similar accuracy?

idea to use these simple well defined final states as the LHC cross section normalisation tool, or standard candle was described first in reference [1]. This study indicated that the W and Z production might result in a precise and simple parton luminosity monitor. In addition, these reactions can also be used to improve the relative knowledge of the PDF's. In fact, if one gives up on the idea to measure absolute cross sections, the relative parton luminosity can in principle be determined with relative uncertainties well below $\pm 5\%$, the previously expected possible limit for any absolute proton-proton luminosity normalisation procedure.

In summary, one can estimate that it should be possible to reduce experimental uncertainties for Drell-Yan processes to systematic uncertainties below $\pm 5\%$, optimistically one might envisage an event counting accuracy of perhaps $\pm 1\%$, limited mainly from the lepton identification efficiency.

The next class of final states, which can be measured exclusively with leptons, are the diboson pair events with subsequent leptonic decays. Starting with the ZZ final state, we expect that the statistical accuracy will dominate the measurement for several years. Nevertheless, the systematic uncertainties of the measurement, based on four leptons, should in principle be possible with relative errors of a few % only.

The production of WZ and WW involves unmeasurable neutrinos. Thus, experimentally only an indirect and incomplete determination of the kinematics of the final states is possible and very detailed simulations with precise Monte Carlo generators are required for the interpretation of these final state. It seems that a measurement of the event counting with an accuracy below $\pm 5\%$, due to efficiency uncertainties from the selection alone, to be highly non trivial. Nevertheless, if the measurements and the interpretations can be done relative to the W and Z resonance production, some uncertainties from the lepton identification efficiency, from the PDF and from the theoretical calculation can perhaps be reduced. Without going into detailed studies for each channel, one could try to assume that a systematic uncertainty of $\pm 5\%$ might be defined as a goal. Similar characteristics and thus limitations can be expected for other diboson signatures.

The production cross section of top antitop quark pairs is large and several million of semileptonic tagged and relatively clean events ($pp \rightarrow t\bar{t} \rightarrow WbWb$ identified with one leptonic W decay) can be expected. However, the signature involves several jets, some perhaps tagged as b-flavoured, and missing transverse momentum from the neutrino(s). The correct association of the various jets to the

corresponding top quark is known to be extremely difficult, leading to large combinatorial backgrounds. Thus, it seems that, even if precise Monte Carlo generators will become eventually available, that systematic uncertainties smaller than 5-10% should not be expected. Consequently, we assume that top antitop backgrounds for a wide class of signals can not be determined with uncertainties smaller than 5-10%.

Measurements of so called “single” top quarks are even more difficult, as the cross section is smaller and larger backgrounds exist. Systematic errors will therefore always be larger than the one guessed for top-antitop pair production.

Finally, we can address the QCD jet production. Traditionally one measures and interprets the so called jet cross section as a function of p_t jet and the mass of the multi jet system using various rapidity intervals. With the steeply falling p_t jet spectrum and essentially no background, one will determine the differential spectrum such that only the slope has to be measured with good relative accuracy. If one is especially interested into the super high mass or high p_t events, then we expect that migrations due to jet mis-measurements and non Gaussian tails in the jet energy measurements will limit any measurement. A good guess might be that the LHC experiments can expect absolute normalisation uncertainties similar to the ones achieved with CDF and D0, corresponding to uncertainties of about ± 10 -20%.

Are the above estimated systematic limits for the various measurements pessimistic, optimistic or simply realistic? Of course, only real experiments will tell during the coming LHC years. However, while some of these estimates will need perhaps some small modification, they could be used as a limit waiting to be improved during the coming years. Thus, some people full of ideas might take these numbers as a challenge, and discover and develop new methods that will improve these estimates. This guess of systematic limitations for LHC experiments could thus be considered as a “provocation”, which will stimulate activities to prove them wrong. In fact, if the experimental and theoretical communities could demonstrate why some of these “pessimistic” numbers are wrong the future real LHC measurements will obviously benefit from the required efforts to develop better Monte Carlo programs and better experimental methods.

The following summary from a variety of experimental results from previous high energy collider experiments might help to quantify particular areas of concern for the LHC measurements. These previous measurements can thus be used as a starting point for an LHC experimenter, who can study and explain why the corresponding errors at LHC will be smaller or larger.

1.2.2 *Learning from previous collider experiments*

It is broadly accepted, due to the huge hadronic interaction rate and the short bunch crossing time, that the experimental conditions at the LHC will be similar or worse than the ones at the Tevatron collider. One experimental answer was to improve the granularity, speed and accuracy of the different detector elements accordingly. Still, no matter how well an experiment can be realized, the LHC conditions to do experiments will be much more difficult than at LEP or any hypothetical future high energy e^+e^- collider. One important reason is the large theoretical uncertainty, which prevents to make signal and background Monte Carlos with accuracies similar to the ones which were used at LEP.

Thus, we can safely expect that systematic errors at LHC experiments will be larger than the corresponding ones from LEP and that the Tevatron experience can be used as a first guess.

- Measurement of $\sigma \times \text{BR}$ for W and Z production from CDF [2] and D0 [3]:
The CDF collaboration has presented a high statistics measurement with electrons and muons. Similar systematic errors of about $\pm 2\%$ were achieved for efficiency and thus the event counting with electrons and muons. The error was reduced to $\pm 1.4\%$ for the ratio measurement where some lepton identification efficiencies cancel. Similar errors about $\times 1.5$ -2 larger have been obtained by the corresponding measurements from the D0 experiment.
- Measurement of the cross section for $p\bar{p} \rightarrow Z\gamma(\gamma)$ from D0 [4]:

A total of 138 $ee\gamma$ and 152 $\mu\mu\gamma$ candidate events were selected. The background was estimated to be about 10% with a systematic uncertainty of $\pm 10\text{-}15\%$, mainly from γ -jet misidentification. Using Monte Carlo and a large sample of inclusive Z events, the efficiency uncertainty has been estimated to be $\approx 5\%$ and when the data were used in comparison with the Standard Model prediction another uncertainty of 3.3% originating from PDF's was added.

- Measurement of the $p\bar{p} \rightarrow t\bar{t}$ production cross section from CDF [5]

A recent CDF measurement, using 197 pb^{-1} , obtained a cross section (in pb) of $7.0 +2.4 (-2.1)$ from statistics. This should be compared with $+1.7 (-1.2)$ from systematics, which includes ± 0.4 from the luminosity measurement. Thus, uncertainties from efficiency and background are roughly $\pm 20\%$. It is expected that some of the uncertainties can be reduced with the expected 10 fold luminosity increase such that the systematic error will eventually decrease to about $\pm 10\%$, sufficient to be better than the expected theoretical error of $\pm 15\%$.

- A search for Supersymmetry with b-tagged jets from CDF [6]:

This study, using single and double b-tagged events was consistent with background only. However, it was claimed that the background uncertainty was dominated by the systematic error, which probably originated mostly from the b tagging efficiency and the misidentification of b-flavoured jets. The numbers given were 16.4 ± 3.7 events (3.15 from systematics) for the single b-tagged events and 2.6 ± 0.7 events (0.66 from systematics) for the double b-tagged events. These errors originate mainly from the b-tagging efficiency uncertainties, which are found to roughly $\pm 20\text{-}25\%$ for this study of rare events.

- Some "random" selection of recent e^+e^- measurements:

A recent measurement from ALEPH (LEP) of the W branching ratio to $q\bar{q}$ estimated a systematic uncertainty of about $\pm 0.2\%$ [7]. This small uncertainty was possible because many additional constraints could be used.

OPAL has reported a measurement of R_b at LEP II energies, with a systematic uncertainty of $\pm 3.7\%$. Even though this uncertainty could in principle be reduced with higher statistics, one can use it as an indication on how large efficiency uncertainties from b-tagging are already with clean experimental conditions [8]

Recently, ALEPH and DELPHI have presented cross section measurements for $e^+e^- \rightarrow \gamma\gamma$ with systematic errors between 2.2% (ALEPH) [9] and 1.1% (DELPHI) [10]. In both cases, the efficiency uncertainty, mainly from conversions, for this in principle easy signal was estimated to be roughly 1%. In the case of ALEPH an uncertainty of about $\pm 0.8\%$ was found for the background correction.

Obviously, these measurements can only be used, in absence of anything better, as a most optimistic guess for possible systematic limitations at a hadron collider. One might conclude that the systematics from LEP experiments give (1) an optimistic limit for comparable signatures at the LHC and (2) that the results from CDF and D0 should indicate systematics which might be obtained realistically during the early LHC years.

Thus, in summary the following list might be used as a first order guess on achievable LHC systematics⁴.

- "Isolated" muons, electrons and photons can be measured with a small momentum (energy) uncertainty and with an almost perfect angular resolution. The efficiency for $p_t \geq 20 \text{ GeV}$ and $|\eta| \leq 2.5$ will be "high" and can be controlled optimistically to $\pm 1\%$. Some straight forward selection criteria should reduce jet background to small or negligible levels.
- "Isolated" jets with a $p_t \geq 30 \text{ GeV}$ and $|\eta| \leq 4.5$ can be seen with high (veto) efficiency and a small uncertainty from the jet direction measurement. However, it will be very difficult to

⁴Reality will hopefully show new brilliant ideas, which combined with hard work will allow to obtain even smaller uncertainties.

measure the absolute jet energy scale and Non-Gaussian tails will limit the systematics if the jet energy scale is important.

- Measurements of the missing transverse momentum depend on the final state but will in general be a sum of the errors from the lepton and the jet accuracies.

Using these assumptions, the following “optimistic” experimental systematic errors can be used as a guideline:

1. Efficiency uncertainties for isolated leptons and photons with a p_t above 20 GeV can be estimated with a $\pm 1\%$ accuracy.
2. Efficiencies for tagging jets will be accurate to a few percent and the efficiency to tag b-flavoured jets will be known at best within $\pm 5\%$.
3. Backgrounds will be known, combining theoretical uncertainties and some experimental determinations, at best with a $\pm 5\text{-}10\%$ accuracy. Thus, discovery signatures without narrow peaks require signal to background ratios larger than 0.25-0.5, if 5σ discoveries are claimed. Obviously, for accurate cross section measurements, the signal to background ratio should be much larger.
4. In case of ratio measurements with isolated leptons, like $pp \rightarrow W^+/\bar{p}p \rightarrow W^-$, relative errors between 0.5-1% should be possible. Furthermore, it seems that the measurement of the shape of Z p_t spectrum, using $Z \rightarrow e^+e^-$, will be possible with a systematic error much smaller than 1%. As the Z cross section is huge and clean we expect that this signature will become the best measurable final state and should allow to test a variety of production models with errors below $\pm 1\%$, thus challenging future QCD calculations for a long time.

1.3 Uncertainties on W and Z production at the LHC⁵

1.3.1 Introduction

At leading order (LO), W and Z production occur by the process, $q\bar{q} \rightarrow W/Z$, and the momentum fractions of the partons participating in this subprocess are given by $x_{1,2} = \frac{M}{\sqrt{s}} \exp(\pm y)$, where M is the centre of mass energy of the subprocess, $M = M_W$ or M_Z , \sqrt{s} is the centre of mass energy of the reaction ($\sqrt{s} = 14$ TeV at the LHC) and $y = \frac{1}{2} \ln \frac{(E+p_t)}{(E-p_t)}$ gives the parton rapidity. The kinematic plane for LHC parton kinematics is shown in Fig. 2. Thus, at central rapidity, the participating partons have small momentum fractions, $x \sim 0.005$. Moving away from central rapidity sends one parton to lower x and one to higher x , but over the measurable rapidity range, $|y| < 2.5$, x values remain in the range, $10^{-4} < x < 0.1$. Thus, in contrast to the situation at the Tevatron, valence quarks are not involved, the scattering is happening between sea quarks. Furthermore, the high scale of the process $Q^2 = M^2 \sim 10,000$ GeV² ensures that the gluon is the dominant parton, see Fig. 2, so that these sea quarks have mostly been generated by the flavour blind $g \rightarrow q\bar{q}$ splitting process. Thus the precision of our knowledge of W and Z cross-sections at the LHC is crucially dependent on the uncertainty on the momentum distribution of the gluon.

HERA data have dramatically improved our knowledge of the gluon, as illustrated in Fig. 3, which shows W and Z rapidity spectra predicted from a global PDF fit which does not include the HERA data, compared to a fit including HERA data. The latter fit is the ZEUS-S global fit [11], whereas the former is a fit using the same fitting analysis but leaving out the ZEUS data. The full PDF uncertainties for both fits are calculated from the error PDF sets of the ZEUS-S analysis using LHAPDF [12] (see the contribution of M. Whalley to these proceedings). The predictions for the W/Z cross-sections, decaying to the lepton decay mode, are summarised in Table 1. The uncertainties in the predictions for these cross-sections have decreased from $\sim 16\%$ pre-HERA to $\sim 3.5\%$ post-HERA. The reason for this can be seen clearly

⁵Contributing authors: Alessandro Tricoli, Amanda Cooper-Sarkar, Claire Gwenlan

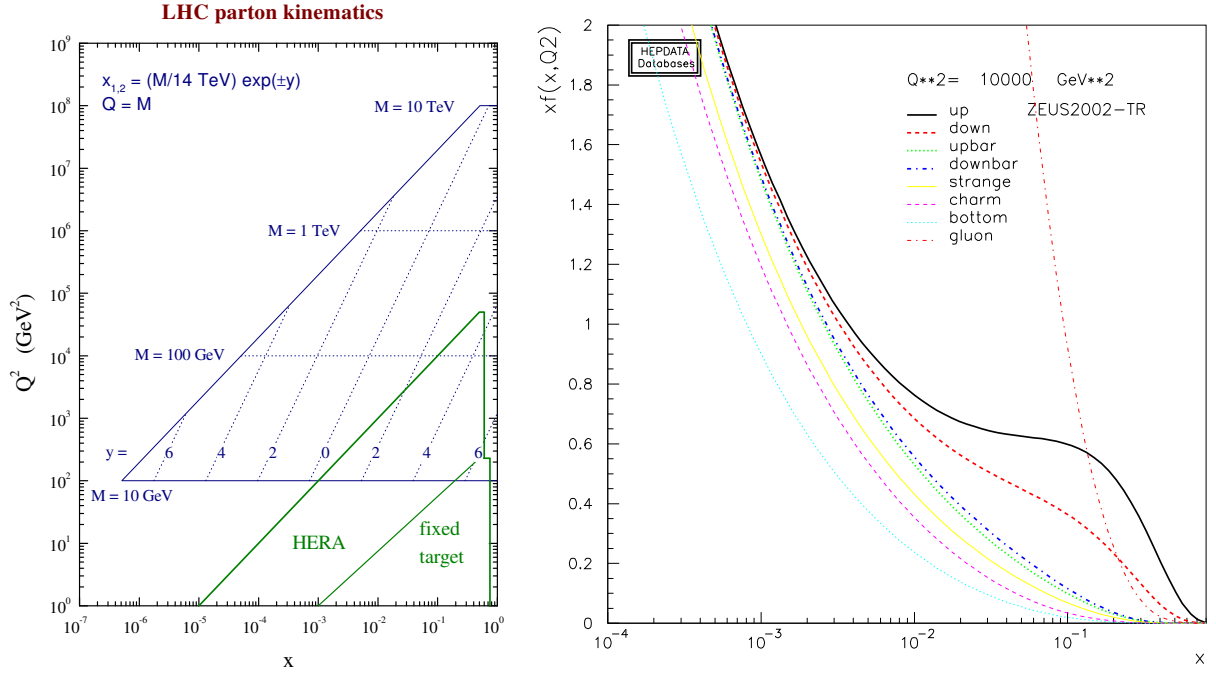


Fig. 2: Left plot: The LHC kinematic plane (thanks to James Stirling). Right plot: PDF distributions at $Q^2 = 10,000 \text{ GeV}^2$.

Table 1: LHC W/Z cross-sections for decay via the lepton mode, for various PDFs

| PDF Set | $\sigma(W^+).B(W^+ \rightarrow l^+\nu_l)$ | $\sigma(W^-).B(W^- \rightarrow l^-\bar{\nu}_l)$ | $\sigma(Z).B(Z \rightarrow l^+l^-)$ |
|----------------|---|---|-------------------------------------|
| ZEUS-S no HERA | $10.63 \pm 1.73 \text{ nb}$ | $7.80 \pm 1.18 \text{ nb}$ | $1.69 \pm 0.23 \text{ nb}$ |
| ZEUS-S | $12.07 \pm 0.41 \text{ nb}$ | $8.76 \pm 0.30 \text{ nb}$ | $1.89 \pm 0.06 \text{ nb}$ |
| CTEQ6.1 | $11.66 \pm 0.56 \text{ nb}$ | $8.58 \pm 0.43 \text{ nb}$ | $1.92 \pm 0.08 \text{ nb}$ |
| MRST01 | $11.72 \pm 0.23 \text{ nb}$ | $8.72 \pm 0.16 \text{ nb}$ | $1.96 \pm 0.03 \text{ nb}$ |

in Fig. 4, where the sea and gluon distributions for the pre- and post-HERA fits are shown for several different Q^2 bins, together with their uncertainty bands. It is the dramatically increased precision in the low- x gluon PDF, feeding into increased precision in the low- x sea quarks, which has led to the increased precision on the predictions for W/Z production at the LHC.

Further evidence for the conclusion that the uncertainties on the gluon PDF at the input scale ($Q_0^2 = 7 \text{ GeV}^2$, for ZEUS-S) are the major contributors to the uncertainty on the W/Z cross-sections at $Q^2 = M_W(M_Z)$, comes from decomposing the predictions down into their contributing eigenvectors. Fig 5 shows the dominant contributions to the total uncertainty from eigenvectors 3, 7, and 11 which are eigenvectors which are dominated by the parameters which control the low- x , mid- x and high- x , gluon respectively.

The post-HERA level of precision illustrated in Fig. 3 is taken for granted in modern analyses, such that W/Z production have been suggested as ‘standard-candle’ processes for luminosity measurement. However, when considering the PDF uncertainties on the Standard Model (SM) predictions it is necessary not only to consider the uncertainties of a particular PDF analysis, but also to compare PDF analyses. Fig. 6 compares the predictions for W^+ production for the ZEUS-S PDFs with those of the CTEQ6.1 [13] PDFs and the MRST01 [14] PDFs⁶. The corresponding W^+ cross-sections, for decay to leptonic mode

⁶MRST01 PDFs are used because the full error analysis is available only for this PDF set.

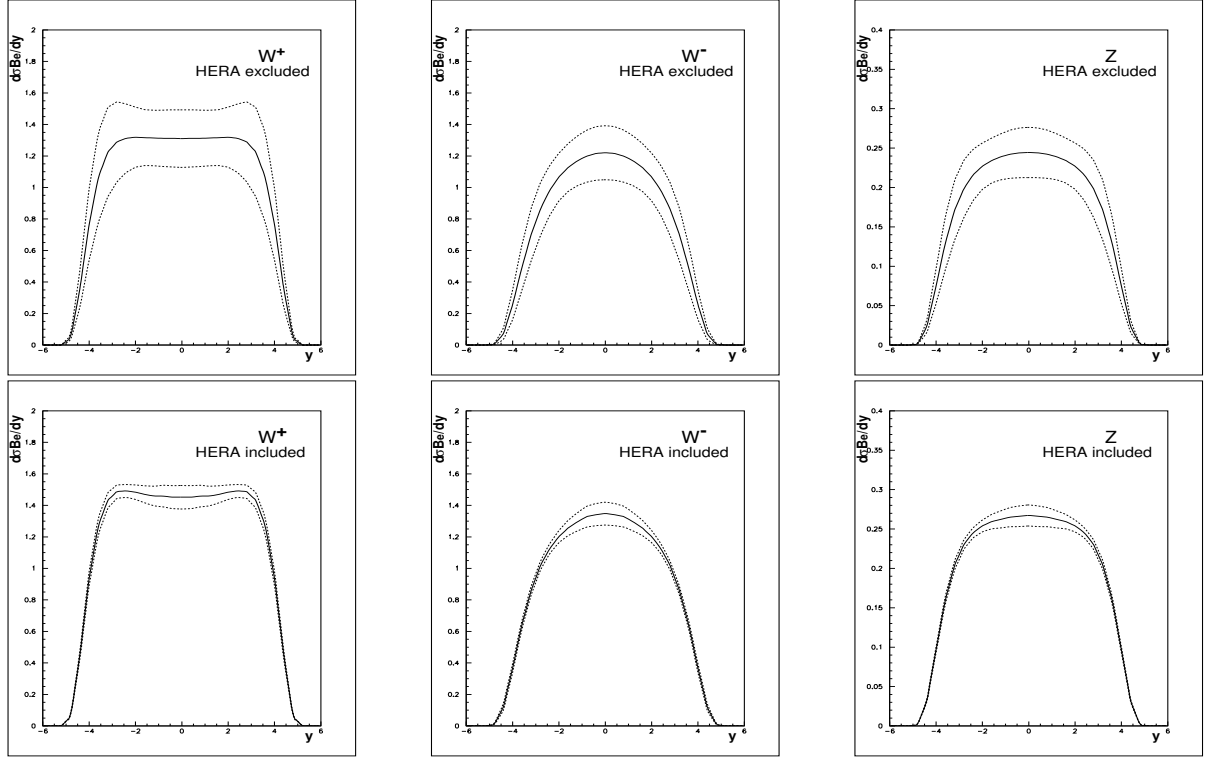


Fig. 3: LHC W^+ , W^- , Z rapidity distributions and their PDF uncertainties (the full line shows the central value and the dashed lines show the spread of the uncertainty): Top Row: from the ZEUS-S global PDF analysis not including HERA data; left plot W^+ ; middle plot W^- ; right plot Z : Bottom Row: from the ZEUS-S global PDF analysis including HERA data; left plot W^+ ; middle plot W^- ; right plot Z

are given in Table 1. Comparing the uncertainty at central rapidity, rather than the total cross-section, we see that the uncertainty estimates are rather larger: 5.2% for ZEUS-S; 8.7% for CTEQ6.1M and about 3.6% for MRST01. The difference in the central value between ZEUS-S and CTEQ6.1 is 3.5%. Thus the spread in the predictions of the different PDF sets is comparable to the uncertainty estimated by the individual analyses. Taking all of these analyses together the uncertainty at central rapidity is about 8%.

Since the PDF uncertainty feeding into the W^+ , W^- and Z production is mostly coming from the gluon PDF, for all three processes, there is a strong correlation in their uncertainties, which can be removed by taking ratios. Fig. 7 shows the W asymmetry

$$A_W = (W^+ - W^-)/(W^+ + W^-).$$

for CTEQ6.1 PDFs, which have the largest uncertainties of published PDF sets. The PDF uncertainties on the asymmetry are very small in the measurable rapidity range. An eigenvector decomposition indicates that sensitivity to high- x u and d quark flavour distributions is now evident at large y . Even this residual flavour sensitivity can be removed by taking the ratio

$$A_{ZW} = Z/(W^+ + W^-)$$

as also shown in Fig. 7. This quantity is almost independent of PDF uncertainties. These quantities have been suggested as benchmarks for our understanding of Standard Model Physics at the LHC. However, whereas the Z rapidity distribution can be fully reconstructed from its decay leptons, this is not possible for the W rapidity distribution, because the leptonic decay channels which we use to identify the W 's

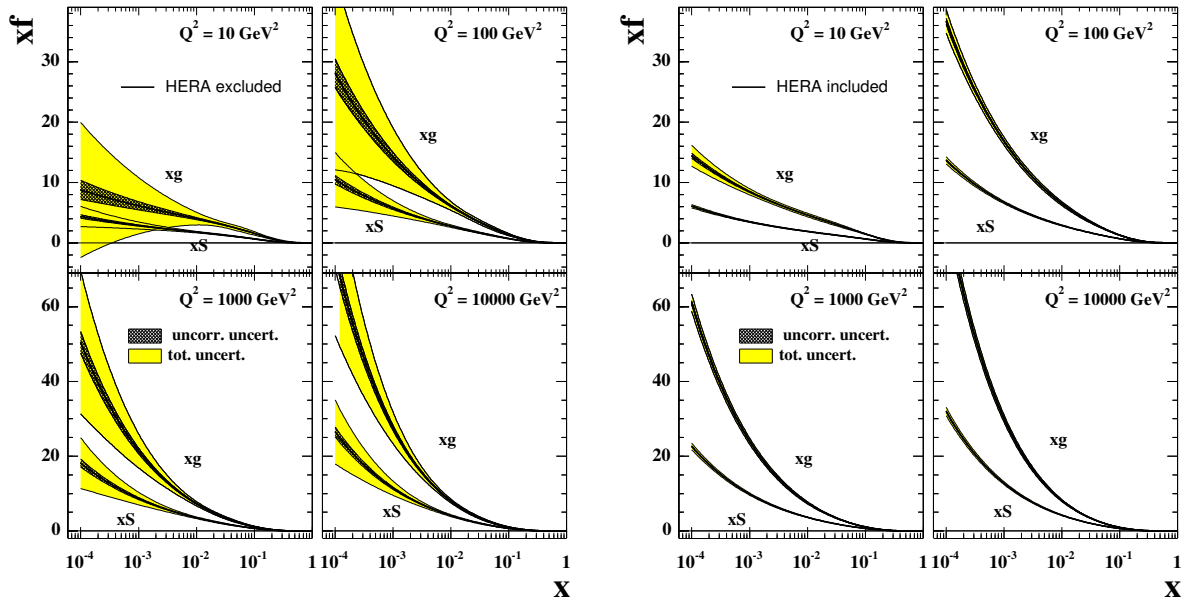


Fig. 4: Sea (xS) and gluon (xg) PDFs at various Q^2 : left plot; from the ZEUS-S global PDF analysis not including HERA data; right plot: from the ZEUS-S global PDF analysis including HERA data. The inner cross-hatched error bands show the statistical and uncorrelated systematic uncertainty, the outer error bands show the total uncertainty including experimental correlated systematic uncertainties, normalisations and model uncertainty.

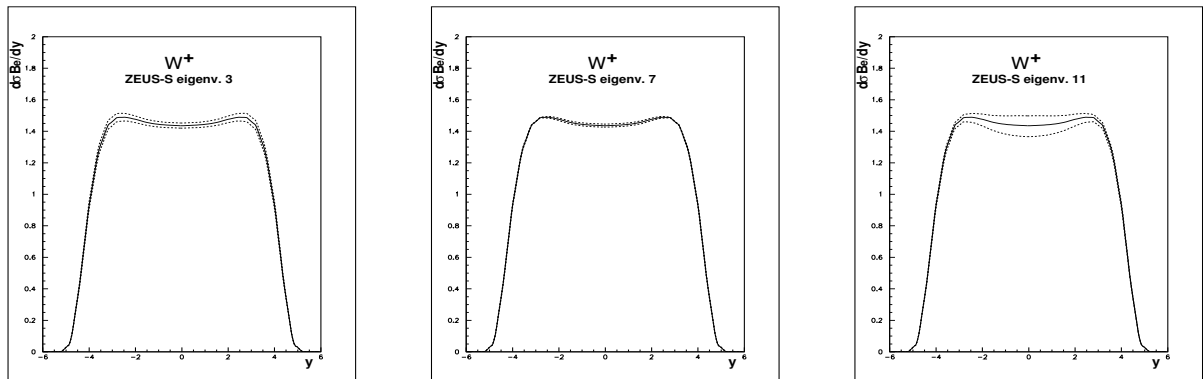


Fig. 5: LHC W^+ rapidity distributions and their PDF uncertainties due to the eigenvectors 3,7 and 11 of the ZEUS-S analysis.

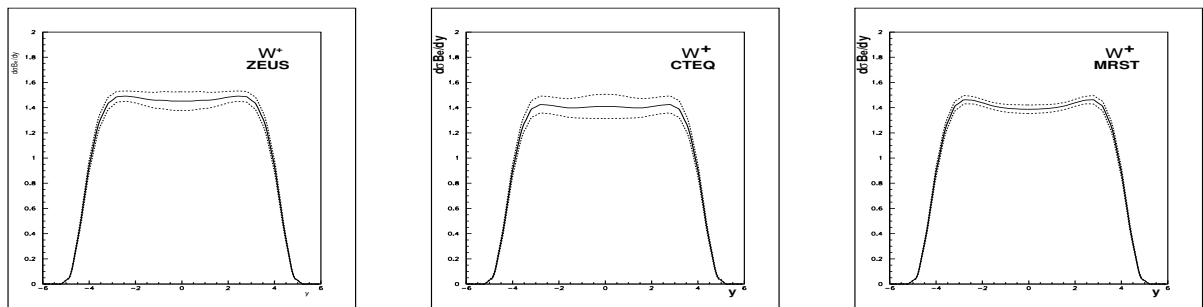


Fig. 6: LHC W^+ rapidity distributions and their PDF uncertainties: left plot, ZEUS-S PDFs; middle plot, CTEQ6.1 PDFs; right plot, MRST01 PDFs.

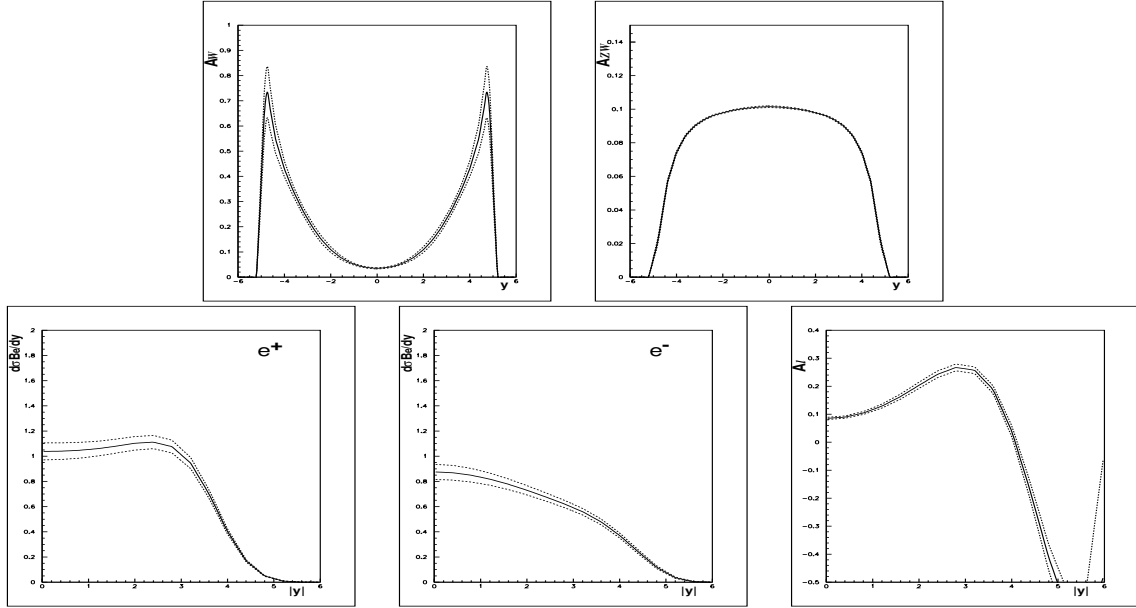


Fig. 7: Predictions for W, Z production at the LHC from the CTEQ6.1 PDFs. Top row: left plot, the W asymmetry, A_W ; right plot, the ratio, A_{ZW} : Bottom row: left plot, decay e^+ rapidity spectrum; middle plot, decay e^- rapidity spectrum; right plot, lepton asymmetry, A_e

have missing neutrinos. Thus we actually measure the W 's decay lepton rapidity spectra rather than the W rapidity spectra. The lower half of Fig. 7 shows the rapidity spectra for positive and negative leptons from W^+ and W^- decay and the lepton asymmetry,

$$A_l = (l^+ - l^-)/(l^+ + l^-).$$

A cut of, $p_{t_l} > 25$ GeV, has been applied on the decay lepton, since it will not be possible to trigger on leptons with small p_{t_l} . A particular lepton rapidity can be fed from a range of W rapidities so that the contributions of partons at different x values is smeared out in the lepton spectra, but the broad features of the W spectra and the sensitivity to the gluon parameters remain. The lepton asymmetry shows the change of sign at large y which is characteristic of the $V - A$ structure of the lepton decay. The cancellation of the uncertainties due to the gluon PDF is not so perfect in the lepton asymmetry as in the W asymmetry. Nevertheless in the measurable rapidity range sensitivity to PDF parameters is small. Correspondingly, the PDF uncertainties are also small (4%) and this quantity provides a suitable Standard Model benchmark.

In summary, these preliminary investigations indicate that PDF uncertainties on predictions for the W, Z rapidity spectra, using standard PDF sets which describe all modern data, have reached a precision of $\sim 8\%$. This may be good enough to consider using these processes as luminosity monitors. The predicted precision on ratios such as the lepton ratio, A_l , is better ($\sim 4\%$) and this measurement may be used as a SM benchmark. It is likely that this current level of uncertainty will have improved before the LHC turns on- see the contribution of C. Gwenlan ([15]) to these proceedings. The remainder of this contribution will be concerned with the question: how accurately can we measure these quantities and can we use the early LHC data to improve on the current level of uncertainty?

1.3.2 k -factor and PDF re-weighting

To investigate how well we can really measure W production we need to generate samples of Monte-Carlo (MC) data and pass them through a simulation of a detector. Various technical problems arise.

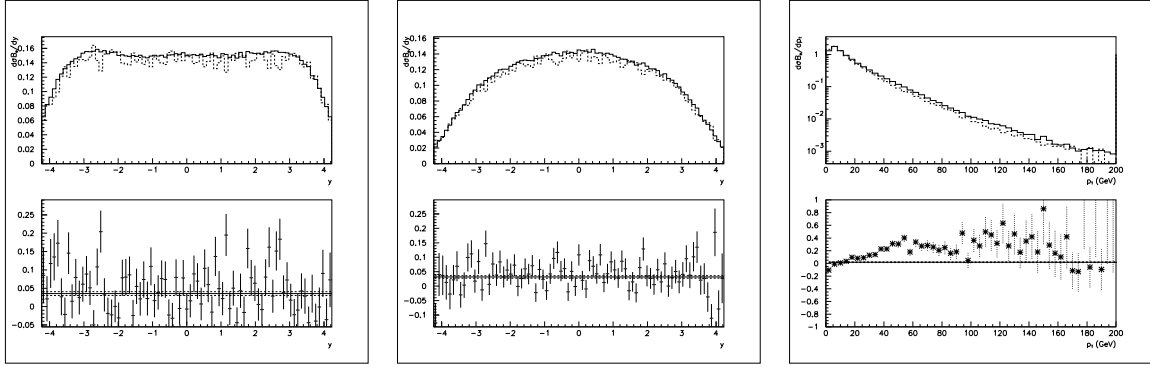


Fig. 8: Top Row: W rapidity and p_t spectra for events generated with HERWIG + k-Factors (full line), compared to those generated by MC@NLO (dashed line); left plot W^+ rapidity; middle plot W^- rapidity; right plot $W^- p_t$. Bottom row: the fractional differences of the spectra generated by HERWIG + k-factors and those generated by MC@NLO. The full line represents the weighted mean of these difference spectra and the dashed lines show its uncertainty

Firstly, many physics studies are done with HERWIG (6.505) [16], which generates events at LO with parton showers to account for higher order effects. Distributions can be corrected from LO to NLO by k-factors which are applied as a function of the variable of interest. The use of HERWIG is gradually being superseded by MC@NLO (2.3) [17] but this is not yet implemented for all physics processes. Thus it is necessary to investigate how much bias is introduced by using HERWIG with k-factors. Secondly, to simulate the spread of current PDF uncertainties, it is necessary to run the MC with all of the eigenvector error sets of the PDF of interest. This would be unreasonably time-consuming. Thus the technique of PDF reweighting has been investigated.

One million $W \rightarrow e\nu_e$ events were generated using HERWIG (6.505). This corresponds to 43 hours of LHC running at low luminosity, $10fb^{-1}$. The events are split into W^+ and W^- events according to their Standard Model cross-section rates, 58%: 42% (the exact split depends on the input PDFs). These events are then weighted with k-factors, which are analytically calculated as the ratio of the NLO to LO cross-section as a function of rapidity for the same input PDF [18]. The resultant rapidity spectra for W^+ , W^- are compared to rapidity spectra for $\sim 107,700$ events generated using MC@NLO(2.3) in Fig 8⁷. The MRST02 PDFs were used for this investigation. The accuracy of this study is limited by the statistics of the MC@NLO generation. Nevertheless it is clear that HERWIG with k-factors does a good job of mimicking the NLO rapidity spectra. However, the normalisation is too high by 3.5%. This is not surprising since, unlike the analytic code, HERWIG is not a purely LO calculation, parton showering is also included. This normalisation difference is not too crucial since in an analysis on real data the MC will only be used to correct data from the detector level to the generator level. For this purpose, it is essential to model the shape of spectra to understand the effect of experimental cuts and smearing but not essential to model the overall normalisation perfectly. However, one should note that HERWIG with k-factors is not so successful in modelling the shape of the p_t spectra, as shown in the right hand plot of Fig. 8. This is hardly surprising, since at LO the W have no p_t and non-zero p_t for HERWIG is generated by parton showering, whereas for MC@NLO non-zero p_t originates from additional higher order processes which cannot be scaled from LO, where they are not present.

Suppose we generate W events with a particular PDF set: PDF set 1. Any one event has the hard scale, $Q^2 = M_W^2$, and two primary partons of flavours $flav_1$ and $flav_2$, with momentum fractions

⁷In MC@NLO the hard emissions are treated by NLO computations, whereas soft/collinear emissions are handled by the MC simulation. In the matching procedure a fraction of events with negative weights is generated to avoid double counting. The event weights must be applied to the generated number of events before the effective number of events can be converted to an equivalent luminosity. The figure given is the effective number of events.

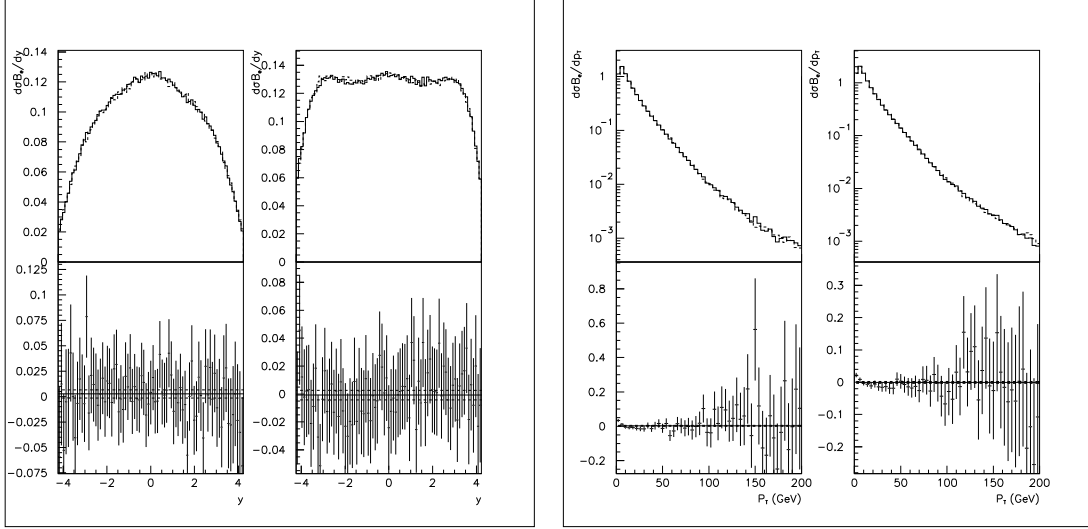


Fig. 9: Left side: W^- (left) and W^+ (right) rapidity spectra, for events generated with MRST02 PDFs reweighted to CTEQ6.1 PDFs (full line), compared to events generated directly with CTEQ6.1 PDFs (dashed line). The fractional difference between these spectra are also shown beneath the plots. The full line represents the weighted mean of these difference spectra and the dashed lines show its uncertainty. Right side: the same for p_t spectra.

x_1, x_2 according to the distributions of PDF set 1. These momentum fractions are applicable to the hard process before the parton showers are implemented in backward evolution in the MC. One can then evaluate the probability of picking up the same flavoured partons with the same momentum fractions from an alternative PDF set, PDF set 2, at the same hard scale. Then the event weight is given by

$$\text{PDF(re-weight)} = \frac{f_{\text{PDF}_2}(x_1, \text{flav}_1, Q^2) \cdot f_{\text{PDF}_2}(x_2, \text{flav}_2, Q^2)}{f_{\text{PDF}_1}(x_1, \text{flav}_1, Q^2) \cdot f_{\text{PDF}_1}(x_2, \text{flav}_2, Q^2)} \quad (1)$$

where $x f_{\text{PDF}}(x, \text{flav}, Q^2)$ is the parton momentum distribution for flavour, flav , at scale, Q^2 , and momentum fraction, x . Fig. 9 compares the W^+ and W^- spectra for a million events generated using MRST02 as PDF set 1 and re-weighting to CTEQ6.1 as PDF set 2, with a million events which are directly generated with CTEQ6.1. Beneath the spectra the fractional difference between these distributions is shown. These difference spectra show that the reweighting is good to better than 1%, and there is no evidence of a y dependent bias. This has been checked for reweighting between MRST02, CTEQ6.1 and ZEUS-S PDFs. Since the uncertainties of any one analysis are similar in size to the differences between the analyses it is clear that the technique can be used to produce spectra for the eigenvector error PDF sets of each analysis and thus to simulate the full PDF uncertainties from a single set of MC generated events. Fig. 9 also shows a similar comparison for p_t spectra.

1.3.3 Background Studies

To investigate the accuracy with which W events can be measured at the LHC it is necessary to make an estimate of the importance of background processes. We focus on W events which are identified through their decay to the $W \rightarrow e \nu_e$ channel. There are several processes which can be misidentified as $W \rightarrow e \nu_e$. These are: $W \rightarrow \tau \nu_\tau$, with τ decaying to the electron channel; $Z \rightarrow \tau^+ \tau^-$ with at least one τ decaying to the electron channel (including the case when both τ 's decay to the electron channel, but one electron is not identified); $Z \rightarrow e^+ e^-$ with one electron not identified. We have generated one million events for each of these background processes, using HERWIG and CTEQ5L, and compared them to one million signal events generated with CTEQ6.1. We apply event selection criteria designed to eliminate the background preferentially. These criteria are:

Table 2: Reduction of signal and background due to cuts

| Cut | $W \rightarrow e\nu_e$ | | $Z \rightarrow \tau^+\tau^-$ | | $Z \rightarrow e^+e^-$ | | $W \rightarrow \tau\nu_\tau$ | |
|-----------------------------|------------------------|---------|------------------------------|-------|------------------------|-------|------------------------------|-------|
| | e^+ | e^- | e^+ | e^- | e^+ | e^- | e^+ | e^- |
| ATLFAST cuts | 382,902 | 264,415 | 5.5% | 7.9% | 34.7% | 50.3% | 14.8% | 14.9% |
| $ \eta < 2.4$ | 367,815 | 255,514 | 5.5% | 7.8% | 34.3% | 49.4% | 14.7% | 14.8% |
| $p_{te} > 25$ GeV | 252,410 | 194,562 | 0.6% | 0.7% | 12.7% | 16.2% | 2.2% | 2.3% |
| $p_{tmiss} > 25$ GeV | 212,967 | 166,793 | 0.2% | 0.2% | 0.1% | 0.2% | 1.6% | 1.6% |
| No jets with $P_t > 30$ GeV | 187,634 | 147,415 | 0.1% | 0.1% | 0.1% | 0.1% | 1.2% | 1.2% |
| $p_t^{recoil} < 20$ GeV | 159,873 | 125,003 | 0.1% | 0.1% | 0.0% | 0.0% | 1.2% | 1.2% |

- ATLFAST cuts (see Sec. 1.3.5)
- pseudorapidity, $|\eta| < 2.4$, to avoid bias at the edge of the measurable rapidity range
- $p_{te} > 25$ GeV, high p_t is necessary for electron triggering
- missing $E_t > 25$ GeV, the ν_e in a signal event will have a correspondingly large missing E_t
- no reconstructed jets in the event with $p_t > 30$ GeV, to discriminate against QCD background
- recoil on the transverse plane $p_t^{recoil} < 20$ GeV, to discriminate against QCD background

Table 2 gives the percentage of background with respect to signal, calculated using the known relative cross-sections of these processes, as each of these cuts is applied. After, the cuts have been applied the background from these processes is negligible. However, there are limitations on this study from the fact that in real data there will be further QCD backgrounds from $2 \rightarrow 2$ processes involving q, \bar{q}, g in which a final state $\pi^0 \rightarrow \gamma\gamma$ decay mimics a single electron. A preliminary study applying the selection criteria to MC generated QCD events suggests that this background is negligible, but the exact level of QCD background cannot be accurately estimated without passing a very large number of events though a full detector simulation, which is beyond the scope of the current contribution.

1.3.4 Charge misidentification

Clearly charge misidentification could distort the lepton rapidity spectra and dilute the asymmetry A_l .

$$A_{true} = \frac{A_{raw} - F^+ + F^-}{1 - F^- - F^+}$$

where A_{raw} is the measured asymmetry, A_{true} is the true asymmetry, F^- is the rate of true e^- misidentified as e^+ and F^+ is the rate of true e^+ misidentified as e^- . To make an estimate of the importance of charge misidentification we use a sample of $Z \rightarrow e^+e^-$ events generated by HERWIG with CTEQ5L and passed through a full simulation of the ATLAS detector. Events with two or more charged electromagnetic objects in the EM calorimeter are then selected and subject to the cuts; $|\eta| < 2.5$, $p_{te} > 25$ GeV, as usual and, $E/p < 2$, for bremsstrahlung rejection. We then look for the charged electromagnetic pair with invariant mass closest to M_Z and impose the cut, $60 < M_Z < 120$ GeV. Then we tag the charge of the better reconstructed lepton of the pair and check to see if the charge of the second lepton is the same as the first. Assuming that the pair really came from the decay of the Z this gives us a measure of charge misidentification. Fig 10 show the misidentification rates F^+ , F^- as functions of pseudorapidity⁸. These rates are very small. The quantity A_l , can be corrected for charge misidentification applying Barlow's method for combining asymmetric errors [19]. The level of correction is 0.3% in the central region and 0.5% in the more forward regions.

⁸These have been corrected for the small possibility that the better reconstructed lepton has had its charge misidentified as follows. In the central region, $|\eta| < 1$, assume the same probability of misidentification of the first and second leptons, in the more forward regions assume the same rate of first lepton misidentification as in the central region.

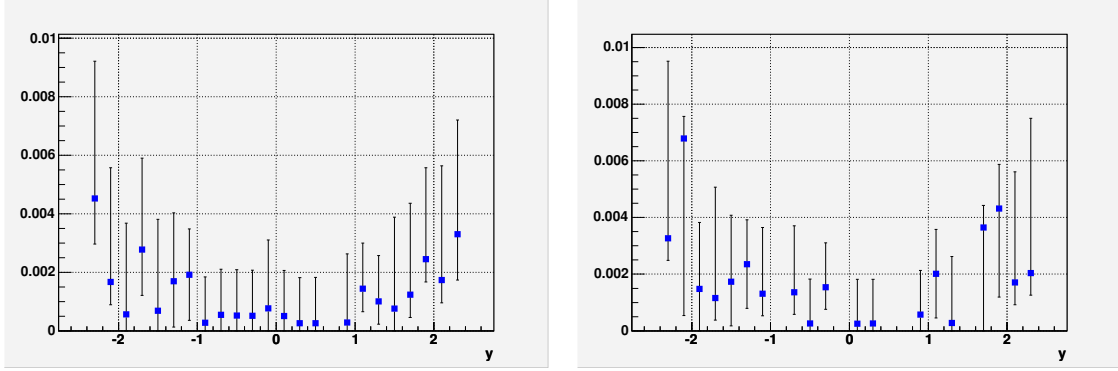


Fig. 10: The rates of charge misidentification as a function of rapidity for e^- misidentified as e^+ (left), e^+ misidentified as e^- (right).

1.3.5 Compare events at the generator level to events at the detector level

We have simulated one million signal, $W \rightarrow e\nu_e$, events for each of the PDF sets CTEQ6.1, MRST2001 and ZEUS-S using HERWIG (6.505). For each of these PDF sets the eigenvector error PDF sets have been simulated by PDF reweighting and k-factors have been applied to approximate an NLO generation. The top part of Fig. 11 shows the e^\pm and A_l spectra at this generator level, for all of the PDF sets superimposed. The events are then passed through the ATLFast fast simulation of the ATLAS detector. This applies loose kinematic cuts: $|\eta| < 2.5$, $p_{te} > 5$ GeV, and electron isolation criteria. It also smears the 4-momenta of the leptons to mimic momentum dependent detector resolution. We then apply the selection cuts described in Sec. 1.3.3. The lower half of Fig. 11 shows the e^\pm and A_l spectra at the detector level after application of these cuts, for all of the PDF sets superimposed. The level of precision of each PDF set, seen in the analytic calculations of Fig. 6, is only slightly degraded at detector level, so that a net level of PDF uncertainty at central rapidity of $\sim 8\%$ is maintained. The anticipated cancellation of PDF uncertainties in the asymmetry spectrum is also observed, within each PDF set, and the spread between PDF sets suggests that measurements which are accurate to better than $\sim 5\%$ could discriminate between PDF sets.

1.3.6 Using LHC data to improve precision on PDFs

The high cross-sections for W production at the LHC ensure that it will be the experimental systematic errors, rather than the statistical errors, which are determining. We have imposed a random 4% scatter on our samples of one million W events, generated using different PDFs, in order to investigate if measurements at this level of precision will improve PDF uncertainties at central rapidity significantly if they are input to a global PDF fit. Fig. 12 shows the e^+ and e^- rapidity spectra for events generated from the ZEUS-S PDFs ($|\eta| < 2.4$) compared to the analytic predictions for these same ZEUS-S PDFs. The lower half of this figure illustrates the result if these events are then included in the ZEUS-S PDF fit. The size of the PDF uncertainties, at $y = 0$, decreases from 5.8% to 4.5%. The largest improvement is in the PDF parameter λ_g controlling the low- x gluon at the input scale, $Q_0^2: xg(x) \sim x^{\lambda_g}$ at low- x , $\lambda_g = -0.199 \pm 0.046$, before the input of the LHC pseudo-data, compared to, $\lambda_g = -0.196 \pm 0.029$, after input. Note that whereas the relative normalisations of the e^+ and e^- spectra are set by the PDFs, the absolute normalisation of the data is free in the fit so that no assumptions are made on our ability to measure luminosity. Secondly, we repeat this procedure for events generated using the CTEQ6.1 PDFs. As shown in Fig. 13, the cross-section for these events is on the lower edge of the uncertainty band of the ZEUS-S predictions. If these events are input to the fit the central value shifts and the uncertainty decreases. The value of the parameter λ_g becomes, $\lambda_g = -0.189 \pm 0.029$, after input of these pseudo-data. Finally to simulate the situation which really faces experimentalists we generate events with CTEQ6.1,

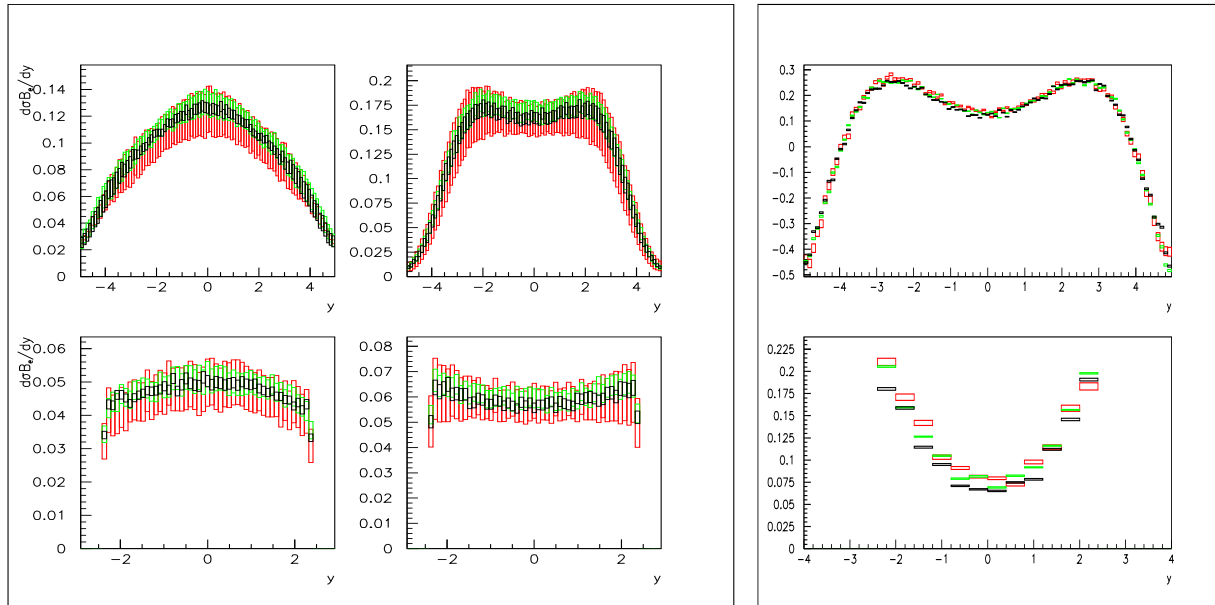


Fig. 11: Top row: e^- , e^+ and A_e rapidity spectra for the lepton from the W decay, generated using HERWIG + k factors and CTEQ6.1 (red), ZEUS-S (green) and MRST2001 (black) PDF sets with full uncertainties. Bottom row: the same spectra after passing through the ATLFast detector simulation and selection cuts.

and pass them through the ATLFast detector simulation and cuts. We then correct back from detector level to generator level using a different PDF set- in this case the ZEUS-S PDFs- since in practice we will not know the true PDFs. Fig. 14 shows that the resulting corrected data look pleasingly like CTEQ6.1, but they are more smeared. When these data are input to the PDF fit the central values shift and errors decrease just as for the perfect CTEQ6.1 pseudo-data. The value of λ_g becomes, $\lambda = -0.181 \pm 0.030$, after input of these pseudo-data. Thus we see that the bias introduced by the correction procedure from detector to generator level is small compared to the PDF uncertainty.

1.3.7 Conclusions and a warning: problems with the theoretical predictions at small- x ?

We have investigated the PDF uncertainty on the predictions for W and Z production at the LHC, taking into account realistic expectations for measurement accuracy and the cuts on data which will be needed to identify signal events from background processes. We conclude that at the present level of PDF uncertainty the decay lepton asymmetry, A_l , will be a useful standard model benchmark measurement, and that the decay lepton spectra can be used as a luminosity monitor which will be good to $\sim 8\%$. However, we have also investigated the measurement accuracy necessary for early measurements of these decay lepton spectra to be useful in further constraining the PDFs. A systematic measurement error of less than $\sim 4\%$ would provide useful extra constraints.

However, a caveat is that the current study has been performed using standard PDF sets which are extracted using NLO QCD in the DGLAP [20–23] formalism. The extension to NNLO is straightforward, giving small corrections $\sim 1\%$. PDF analyses at NNLO including full accounting of the PDF uncertainties are not extensively available yet, so this small correction is not pursued here. However, there may be much larger uncertainties in the theoretical calculations because the kinematic region involves low- x . There may be a need to account for $\ln(1/x)$ resummation (first considered in the BFKL [24–26] formalism) or high gluon density effects. See reference [27] for a review.

The MRST group recently produced a PDF set, MRST03, which does not include any data for $x < 5 \times 10^{-3}$. The motivation behind this was as follows. In a global DGLAP fit to many data sets there is always a certain amount of tension between data sets. This may derive from the use of an inappropriate

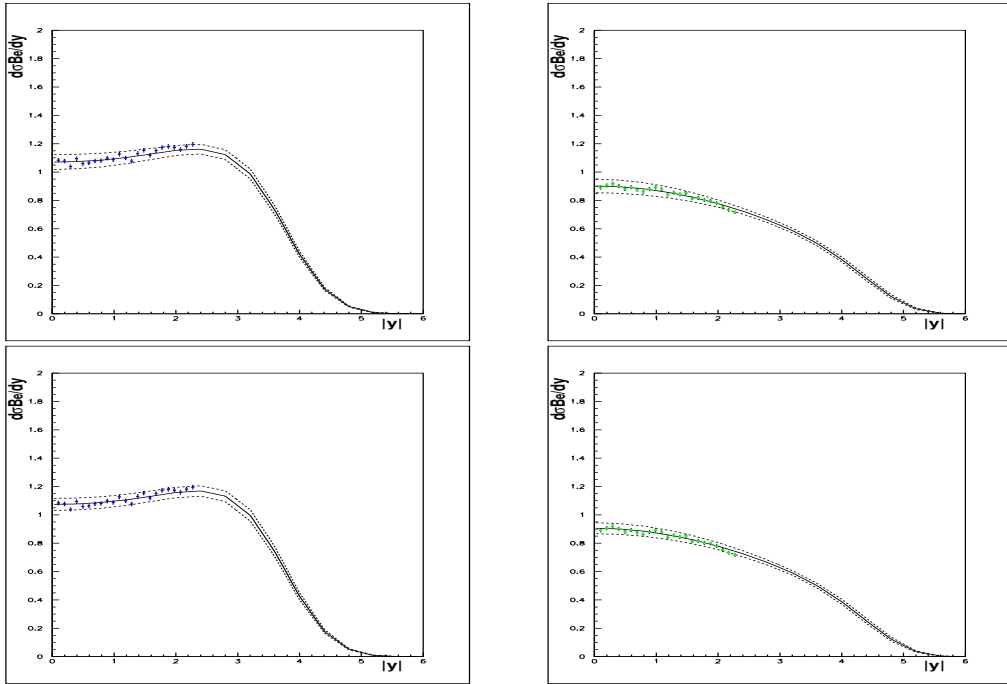


Fig. 12: Top row: e^+ and e^- rapidity spectra generated from ZEUS-S PDFs compared to the analytic prediction using ZEUS-S PDFs. Bottom row: the same lepton rapidity spectra compared to the analytic prediction AFTER including these lepton pseudo-data in the ZEUS-S PDF fit.

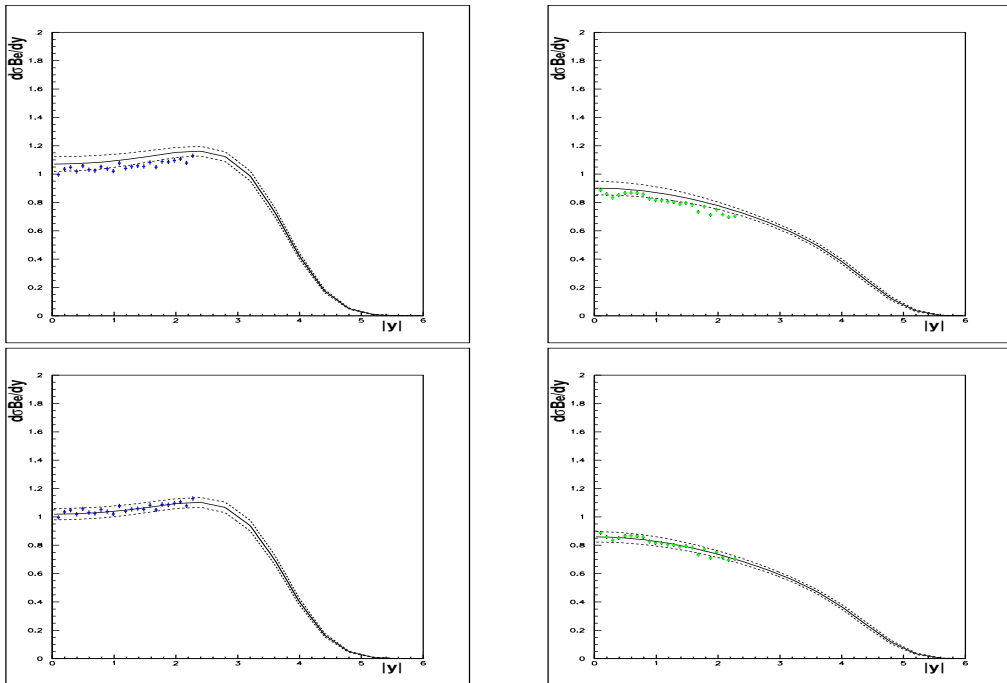


Fig. 13: Top row: e^+ and e^- rapidity spectra generated from CTEQ6.1 PDFs compared to the analytic prediction using ZEUS-S PDFs. Bottom row: the same lepton rapidity spectra compared to the analytic prediction AFTER including these lepton pseudo-data in the ZEUS-S PDF fit.

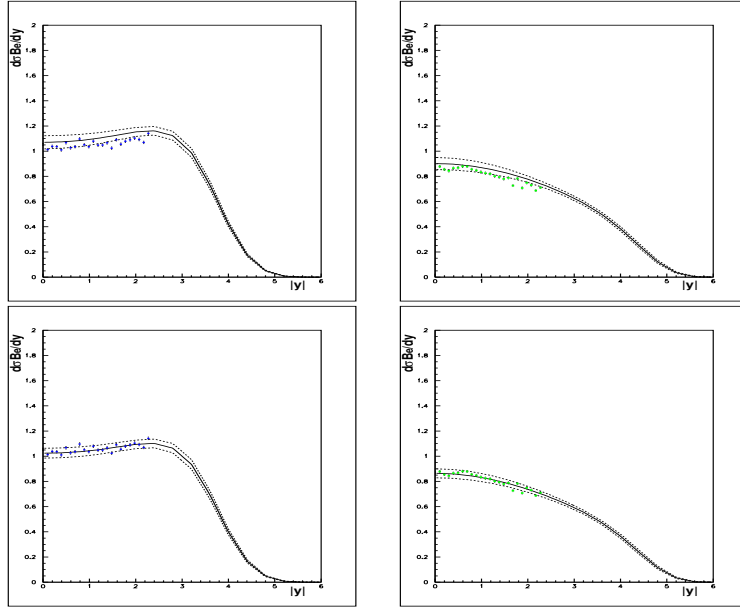


Fig. 14: Top row: e^+ and e^- rapidity spectra generated from CTEQ6.1 PDFs, which have been passed through the ATLFast detector simulation and corrected back to generator level using ZEUS-S PDFs, compared to the analytic prediction using ZEUS-S PDFs. Bottom row: the same lepton rapidity spectra compared to the analytic prediction AFTER including these lepton pseudo-data in the ZEUS-S PDF fit.

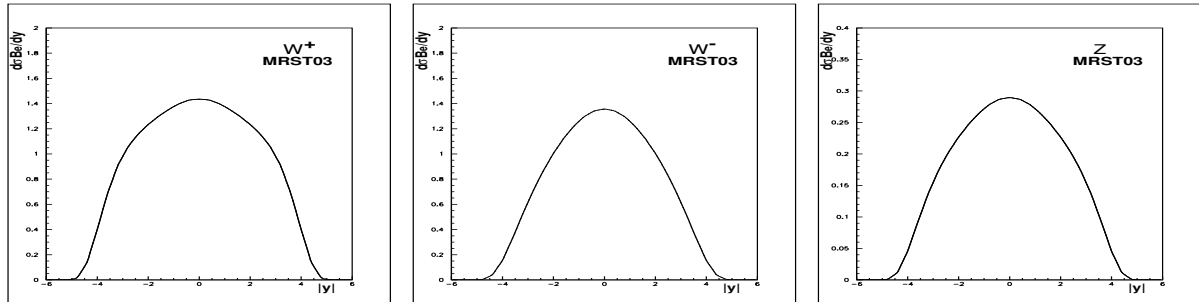


Fig. 15: LHC W^+ , W^- , Z rapidity distributions for MRST03 PDFs: left plot W^+ ; middle plot W^- ; right plot Z

theoretical formalism for the kinematic range of some of the data. Investigating the effect of kinematic cuts on the data, MRST found that a cut, $x > 5 \times 10^{-3}$, considerably reduced tension between the remaining data sets. An explanation may be the inappropriate use of the DGLAP formalism at small- x . The MRST03 PDF set is thus free of this bias BUT it is also only valid to use it for $x > 5 \times 10^{-3}$. What is needed is an alternative theoretical formalism for smaller x . However, the MRST03 PDF set may be used as a toy PDF set, to illustrate the effect of using very different PDF sets on our predictions. A comparison of Fig. 15 with Fig. 3 or Fig. 6 shows how different the analytic predictions are from the conventional ones, and thus illustrates where we might expect to see differences due to the need for an alternative formalism at small- x .

1.4 W and Z production at the LHC ⁹

The study of the production at the LHC of the electroweak bosons W and Z with subsequent decays in leptonic final states will provide several precision measurements of Standard Model parameters such

⁹Contributing author: Hasko Stenzel

as the mass of the W boson or the weak mixing angle from the Z boson forward-backward asymmetry. Given their large cross section and clean experimental signatures, the bosons will furthermore serve as calibration tool and luminosity monitor. More challenging, differential cross sections in rapidity or transverse momentum may be used to further constrain parton distribution functions. Eventually these measurements for single inclusive boson production may be applied to boson pair production in order to derive precision predictions for background estimates to discovery channels like $H \rightarrow W^+W^-$.

This contribution is devoted to the estimation of current uncertainties in the calculations for Standard Model cross sections involving W and Z bosons with particular emphasis on the PDF and perturbative uncertainties. All results are obtained at NLO with MCFM [28] version 4.0 interfaced to LHAPDF [12] for a convenient selection of various PDF families and evaluation of their intrinsic uncertainties. The cross sections are evaluated within a typical experimental acceptance and for momentum cuts summarised in Table 3. The electromagnetic decays of W and Z are considered (massless leptons) and the missing transverse energy is assigned to the neutrino momentum sum (in case of W decays). Jets in the processes $W/Z + jets$ are produced in an inclusive mode with at least one jet in the event

Table 3: Experimental acceptance cuts used for the calculation of cross-sections.

| Observable | cut |
|------------------------------------|--------------------|
| p_T^{lept} | $> 25 \text{ GeV}$ |
| p_T^{jet} | $> 25 \text{ GeV}$ |
| $ \eta_{\text{lept}} $ | < 3.0 |
| $ \eta_{\text{jet}} $ | < 4.0 |
| $R(\text{lepton} - \text{jet})$ | > 0.8 |
| $R(\text{lepton} - \text{lepton})$ | > 0.2 |
| E_T^{miss} | $> 25 \text{ GeV}$ |

reconstructed with the k_T -algorithm. MCFM includes one- and two-jet processes at NLO and three-jet processes at LO. In the case of boson pair production the cuts of Table 3 can only be applied to the two leading leptons, hence a complete acceptance is assumed for additional leptons e.g. from ZZ or WZ decays.

The calculations with MCFM are carried out for a given fixed set of electroweak input parameters using the effective field theory approach [28]. The PDF family CTEQ61 provided by the CTEQ collaboration [29] is taken as nominal PDF input while MRST2001E given by the MRST group [30] is considered for systematic purposes. The difference between CTEQ61 and MRST2001E alone can't be considered as systematic uncertainty but merely as cross-check. The systematic uncertainty is therefore estimated for each family separately with the family members, 40 for CTEQ61 and 30 for MRST2001E, which are variants of the nominal PDF obtained with different assumptions while maintaining a reasonable fit of the input data. The value of α_s is not a free input parameter for the cross section calculation but taken from the corresponding value in the PDF.

Important input parameters are renormalisation and factorisation scales. The central results are obtained with $\mu_R = \mu_F = M_V$, $V = W, Z$ for single boson production and $\mu_R = \mu_F = M_V + M'_V$ for pair production (V' being the second boson in the event). Missing higher orders are estimated by a variation of the scales in the range $1/2 \leq x_{\mu_R} \leq 2$ and independently $1/2 \leq x_{\mu_F} \leq 2$ where $\mu = x_\mu \cdot M_V$, following prescriptions applied to other processes [31], keeping in mind that the range of variation of the scales is purely conventional.

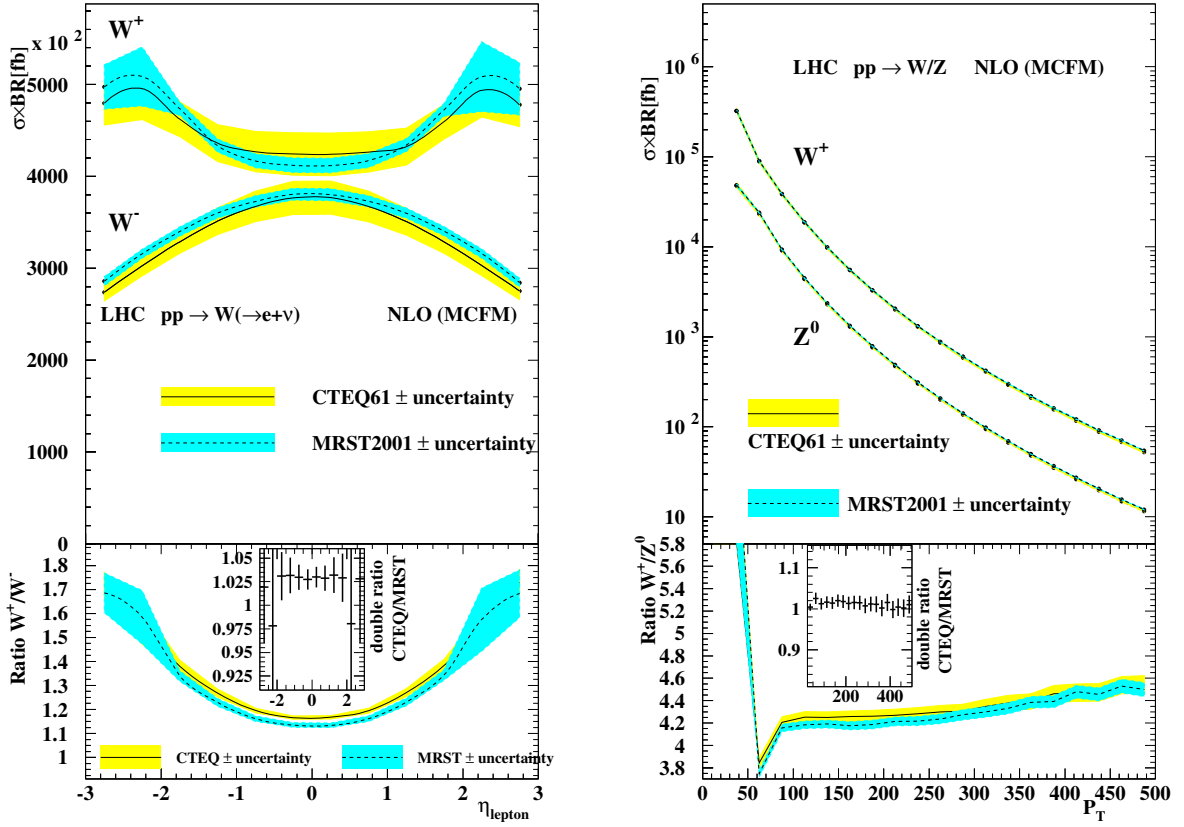


Fig. 16: Left: pseudo-rapidity distribution of the decay lepton from inclusive W production and right: p_T spectra of W and Z . The bands represent the PDF-uncertainty. The lower inserts show on the left side the ratio W^+/W^- resp. the double-ratio CTEQ/MRST and on the right side the ratios for W^+/Z^0 .

1.4.1 Single W and Z cross sections

Detailed studies of single W and Z production including detector simulation are presented elsewhere in these proceedings, here these channels are mainly studied for comparison with the associated production with explicitly reconstructed jets and with pair production. The selected process is inclusive in the sense that additional jets, present in the NLO calculation, are not explicitly reconstructed. The experimentally required lepton isolation entailing a jet veto in a restricted region of phase space is disregarded at this stage.

As an example the pseudo-rapidity distribution of the lepton from W decays and the p_T spectra for Z and W^+ are shown in Fig. 16. The cross section for W^+ is larger than for W^- as a direct consequence of the difference between up- and down-quark PDFs, and this difference survives in the pseudo-rapidity distribution of the decay lepton with a maximum around $|\eta|=2.5$. In the central part the PDF uncertainty, represented by the bands in Fig. 16, amounts to about 5% for CTEQ and 2% for MRST, and within the uncertainty CTEQ and MRST are fully consistent. Larger differences are visible in the peaks for the W^+ , where at the same time the PDF uncertainty increases. In the ratio W^+/W^- the PDF uncertainty is reduced to about 1-2% in the central region and a difference of about 3% is observed between CTEQ and MRST, as can be seen from the double-ratio CTEQ/MRST. The uncertainty of the double ratio is calculated from the CTEQ uncertainty band alone.

In the case of Z production the rapidity and p_T spectra can be fully reconstructed from the e^+e^- pair. A measurement of the Z p_T spectrum may be used to tune the Monte Carlo description of W p_T , which is relevant for measurements of the W mass. The p_T spectra are shown in the right part of Fig. 16. The total yield for W^+ is about six times larger than for Z^0 but for $p_T > 150$ GeV the ratio

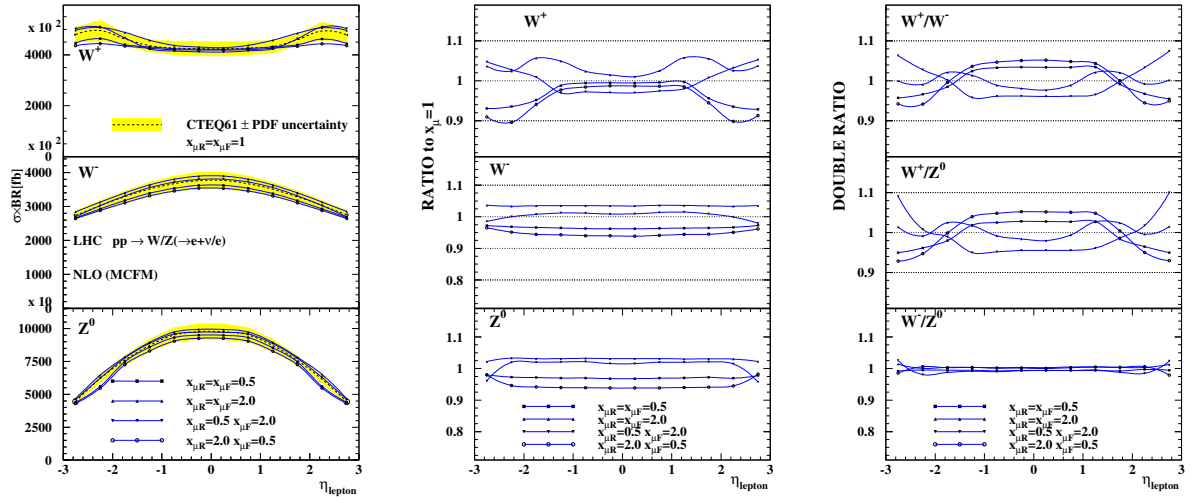


Fig. 17: Left: pseudo-rapidity distribution of the decay lepton from inclusive W/Z production for different values of $x_{\mu R}$ and $x_{\mu F} = 1$, centre: the ratio of predictions with respect to $x_{\mu} = 1$ and right: double ratio V/V' of cross sections for actual scale settings normalised to the nominal scale.

stabilises around 4.5. At small values of p_T the fixed-order calculation becomes trustless and should be supplemented by resummed calculations. The PDF uncertainties for the p_T spectra themselves are again about 5% and about 2% in the ratio, CTEQ and MRST being consistent over the entire p_T range.

The perturbative uncertainties are estimated by variations of the renormalisation and factorisation scales in by a factor of two. The scale variation entails a global change in the total cross section of the order of 5%. The η distribution of leptons from W/Z decays are shown in Fig. 17, comparing the nominal cross section with $x_{\mu R} = x_{\mu F} = 1$, to alternative scale settings. The nominal cross section is drawn with its PDF uncertainty band, illustrating that the perturbative uncertainties are of the same size. For W^- and Z^0 the shape of the distribution is essentially unaltered, but for W^+ the region around the maxima is changed more than the central part, leading to a shape deformation. The scale variation uncertainty is strongly correlated for W^- and Z^0 and cancels in the ratio W^-/Z^0 , but for W^+ it is almost anti-correlated with W^- and Z^0 and partly enhanced in the ratio.

Globally the perturbative uncertainty is dominated by the asymmetric scale setting $x_{\mu R} = 2, x_{\mu F} = 1/2$ for which a change of -5% is observed, the largest upward shift of 3.5% is obtained for $x_{\mu R} = 2, x_{\mu F} = 2$, locally the uncertainty for W^+ can be much different. It can be expected that the perturbative uncertainties are reduced for NNLO calculations to the level of 1%.

The integrated cross sections and systematic uncertainties within the experimental acceptance are summarised in Table 4.

1.4.2 $W/Z + jet$ production

In the inclusive production of $W/Z + jet$ at least one jet is requested to be reconstructed, isolated from any lepton by $R > 0.8$. Additional jets are in case of overlap eventually merged at reconstruction level by the k_T -prescription. Given the presence of a relatively hard ($p_T > 25$ GeV) jet, it can be expected that PDF- and perturbative uncertainties are different than for single boson production. The study of this process at the LHC, other than being a stringent test of perturbative QCD, may in addition contribute to a better understanding of the gluon PDF.

The first difference with respect to single boson production appears in the lepton pseudo-rapidity, shown in Fig. 18. The peaks in the lepton spectrum from W^+ disappeared, the corresponding spectrum

Table 4: Total cross-sections and systematic uncertainties within the experimental acceptance.

| | W^+ | W^- | Z^0 |
|--|-----------|------------|------------|
| CTEQ61 [pb] | 5438 | 4002 | 923.9 |
| $\Delta_{\text{PDF}}^{\text{CTEQ}}$ [pb] | ± 282 | ± 221 | ± 49.1 |
| $\Delta_{\text{PDF}}^{\text{CTEQ}}$ [%] | ± 5.2 | ± 5.5 | ± 5.3 |
| MRST [pb] | 5480 | 4110 | 951.1 |
| $\Delta_{\text{PDF}}^{\text{MRST}}$ [pb] | ± 103 | ± 83.4 | ± 17.4 |
| $\Delta_{\text{PDF}}^{\text{MRST}}$ [%] | ± 1.9 | ± 2.1 | ± 1.9 |
| Δ_{pert} [%] | $+3.5$ | $+3.5$ | $+3.1$ |
| | -5.2 | -5.4 | -5.5 |

Table 5: Total cross-sections and systematic uncertainties within the experimental acceptance for $W/Z + jet$ processes.

| | $W^+ + jet$ | $W^- + jet$ | $Z^0 + jet$ |
|--|-------------|-------------|-------------|
| CTEQ61 [pb] | 1041 | 784.5 | 208.1 |
| $\Delta_{\text{PDF}}^{\text{CTEQ}}$ [pb] | ± 44.1 | ± 34.3 | ± 9.01 |
| $\Delta_{\text{PDF}}^{\text{CTEQ}}$ [%] | ± 4.2 | ± 4.4 | ± 4.3 |
| MRST [pb] | 1046 | 797.7 | 211.3 |
| $\Delta_{\text{PDF}}^{\text{MRST}}$ [pb] | ± 17.6 | ± 14.8 | ± 3.67 |
| $\Delta_{\text{PDF}}^{\text{MRST}}$ [%] | ± 1.7 | ± 1.9 | ± 1.8 |
| Δ_{pert} [%] | $+8.7$ | $+8.9$ | $+7.6$ |
| | -9.8 | -10.0 | -9.1 |

from W^- is stronger peaked at central rapidity while the ratio W^+/W^- with jets is essentially the same as without jets. The PDF uncertainties are slightly smaller (4.2-4.4%) compared to single bosons. The jet pseudo-rapidities are shown in the right part of Fig. 18, they are much stronger peaked in the central region but the ratio W^+/W^- for jets is similar to the lepton ratio.

The transverse momenta of associated jets from $W/Z + jet$ production is shown in Fig. 19, the spectra are steeply falling and the ratio W^+/W^- is increasing from 1.3 at low p_T to almost 2 at 500 GeV p_T .

The perturbative uncertainties are investigated in the same way as for the single boson production and are shown in Fig. 20. The scale variation entails here a much larger uncertainty between 8 and 10%, almost twice as large as for single bosons. In contrast to the latter case, the scale variation is correlated for W and Z and cancels in the ratio W^+/W^- , with an exception for W^- where a bump appears at $|\eta| = 1.8$ for $x_{\mu R} = 2$.

The total cross sections and their systematic uncertainties are summarised in Table 5.

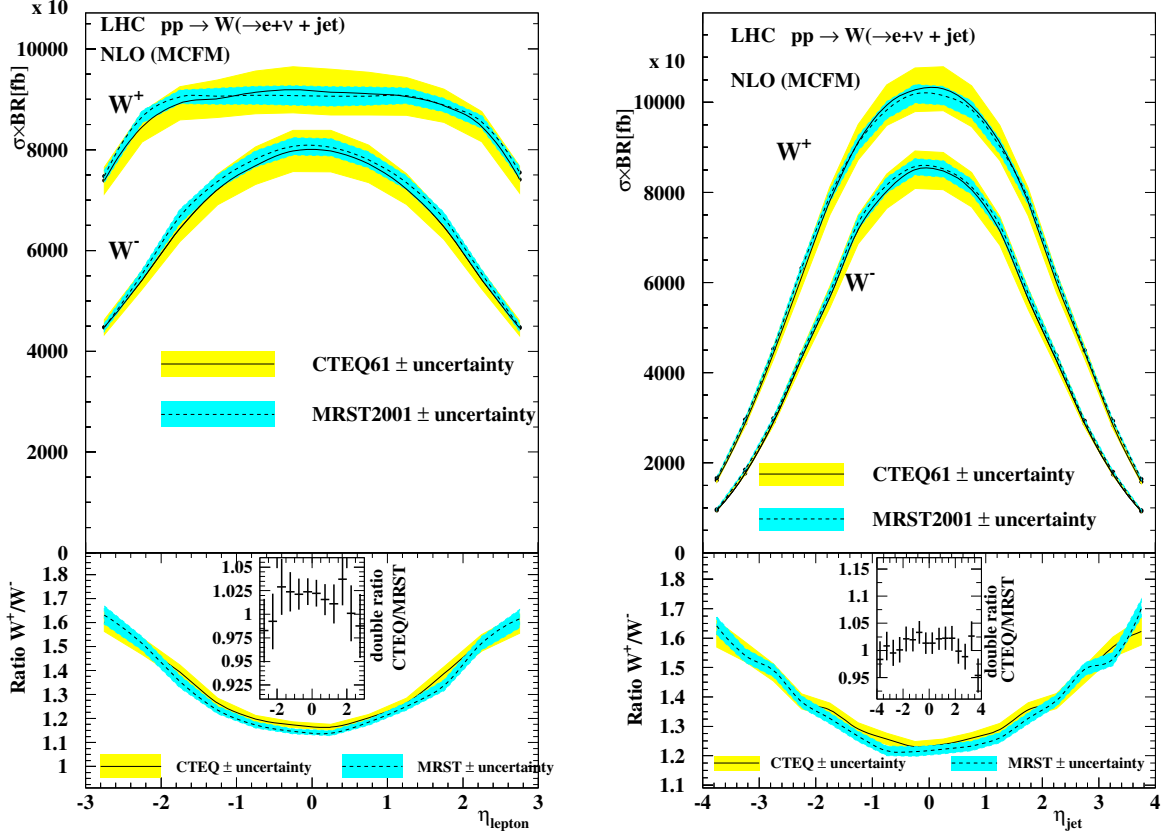


Fig. 18: Left: pseudo-rapidity distribution of the decay lepton from inclusive W +jet production and right: pseudo-rapidity of the associated leading jet. The bands represent the PDF-uncertainty.

1.4.3 Vector Boson pair production

In the Standard Model the non-resonant production of vector bosons pairs in the continuum is suppressed by factors of 10^4 - 10^5 with respect to single Boson production. The cross sections for WW , WZ and ZZ within the experimental acceptance range from 500 fb (WW) to 10 fb (ZZ). Given the expected limited statistics for these processes, the main goal of their experimental study is to obtain the best estimate of the background they represent for searches of the Higgs boson or new physics yielding boson pairs.

The selection of boson pairs follows in extension the single boson selection cuts applied to 2, 3 or 4 isolated leptons. Again real gluon radiation and virtual loops have been taken into account at NLO but without applying lepton-jet isolation cuts. Lepton-lepton separation is considered only for the two leading leptons.

The pseudo-rapidity and transverse momentum distributions taking the e^+ from W^+W^- production as example are shown in Fig. 21. The pseudo-rapidity is strongly peaked and the cross section at $\eta = 0$ twice as large as at $|\eta| = 3$. The PDF uncertainties are smaller than for single bosons, between 3.5 and 4 %.

The same shape of lepton distributions is also found for the other lepton and for the other pair production processes, as shown for the W^-Z^0 case in Fig. 22.

The rapidity distribution of the leading Z^0 from ZZ production is shown in the left part of Fig. 23. With both Z 's being fully reconstructed, the invariant mass of the ZZ system can be compared in the right part of Fig. 23 to the invariant mass spectrum of the Higgs decaying into the same final state for an intermediate mass of $m_H = 200$ GeV. In this case a clear peak appears at low invariant masses above the continuum, and the mass spectrum is also harder at high masses in presence of the Higgs.

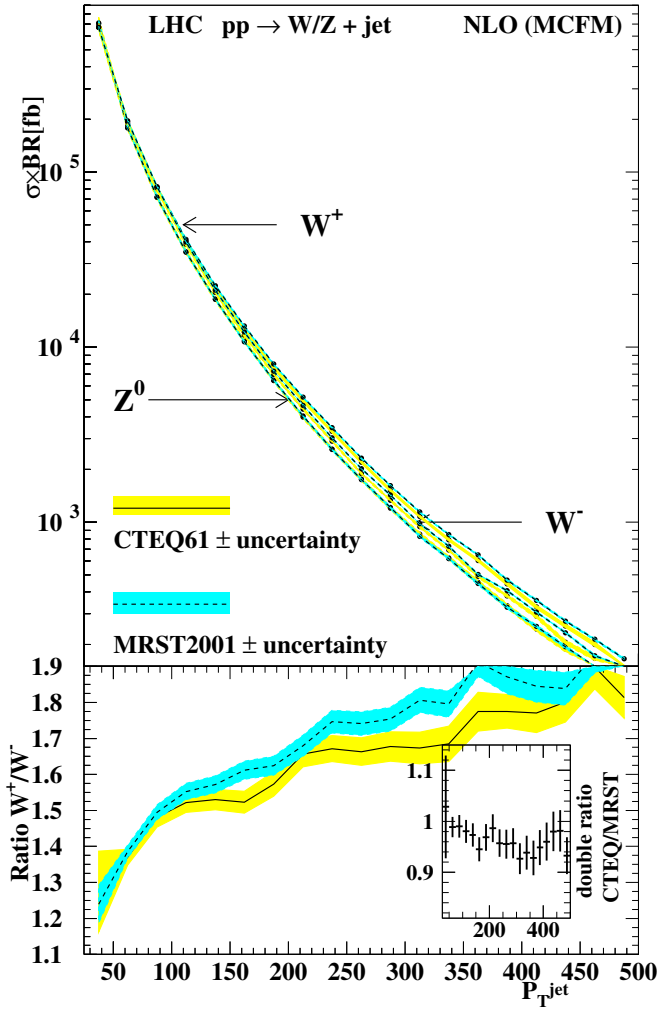


Fig. 19: Transverse momentum distribution of the jet from inclusive $W/Z + \text{jet}$ production

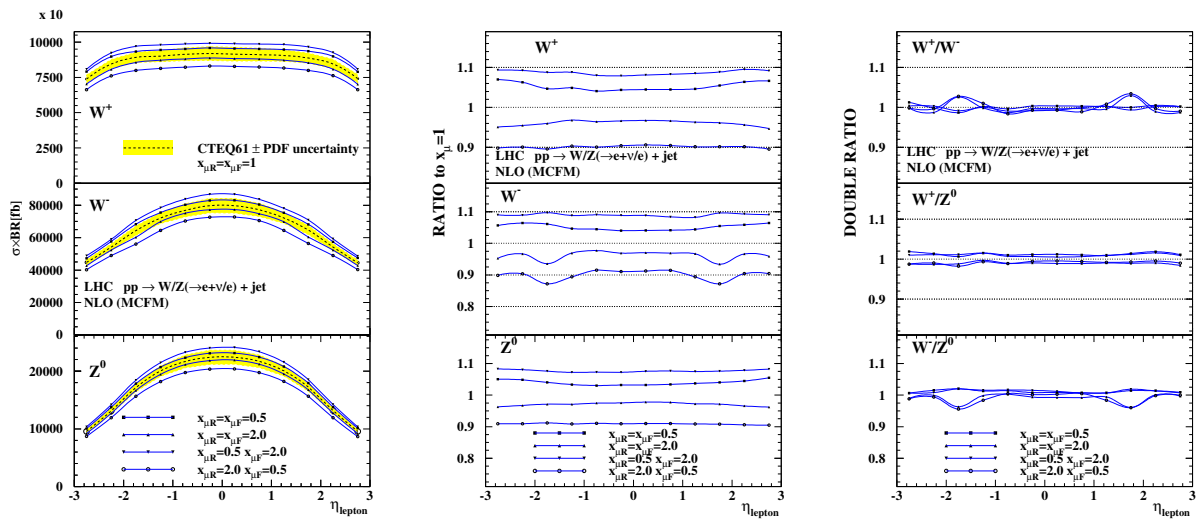


Fig. 20: Left: pseudo-rapidity distribution of the decay lepton from inclusive $W/Z + \text{jet}$ production for different values of $x_{\mu R}$ and $x_{\mu F} = 1$, centre: the ratio of predictions with respect to $x_{\mu} = 1$ and right: double ratio V/V' of cross sections for actual scale settings normalised to the nominal scale.

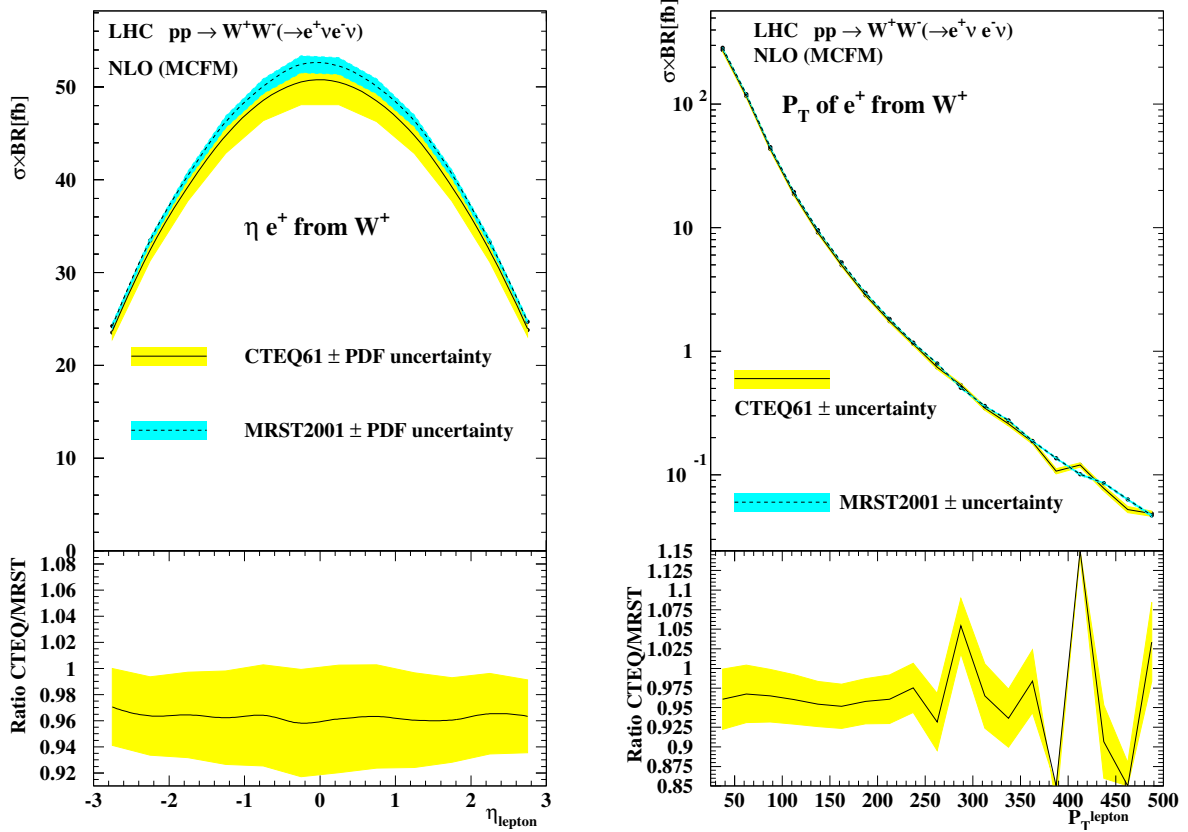


Fig. 21: Left: pseudo-rapidity distribution of the decay lepton from inclusive WW production and right: transverse momentum of the decay lepton.

The perturbative uncertainties, obtained as for the other processes, are shown in Fig. 24 for the lepton distributions. The systematic uncertainties range from 3.3 to 4.9 % and are slightly smaller than for single bosons, given the larger scale $\mu = 2M_V$ and better applicability of perturbative QCD. The perturbative uncertainty is essentially constant across the pseudo-rapidity and largely correlated between different pair production processes.

The ratio of boson pair production to single Z production is of particular interest, as similar quark configurations contribute to both process types, though evidently in a somewhat different x, Q^2 regime. This ratio is shown in Fig. 25 for the lepton distribution, given the different shapes of pseudo-rapidity is not flat but its PDF uncertainty is reduced to the level of 2 %. The perturbative uncertainties of the VV/Z ratio, however, are only reduced for the ZZ/Z case and even slightly larger for other ratios because the scale variations have partly an opposite effect on the cross sections for Z and e.g. WW production.

The total cross sections and their systematic uncertainties are summarised in Table 6.

1.5 Study of next-to-next-to-leading order QCD predictions for W and Z production at LHC¹⁰

It has been in 2004 that the first differential next-to-next-to-leading order (NNLO) QCD calculation for vector boson production in hadron collisions was completed by Anastasiou *et al.* [32]. This group has calculated the rapidity dependence for W and Z production at NNLO. They have shown that the perturbative expansion stabilizes at this order in perturbation theory and that the renormalization and factorization scale uncertainties are drastically reduced, down to the level of one per-cent. It is therefore interesting to perform a more detailed study of these NNLO predictions for various observables which

¹⁰Contributing author:Günther Dissertori

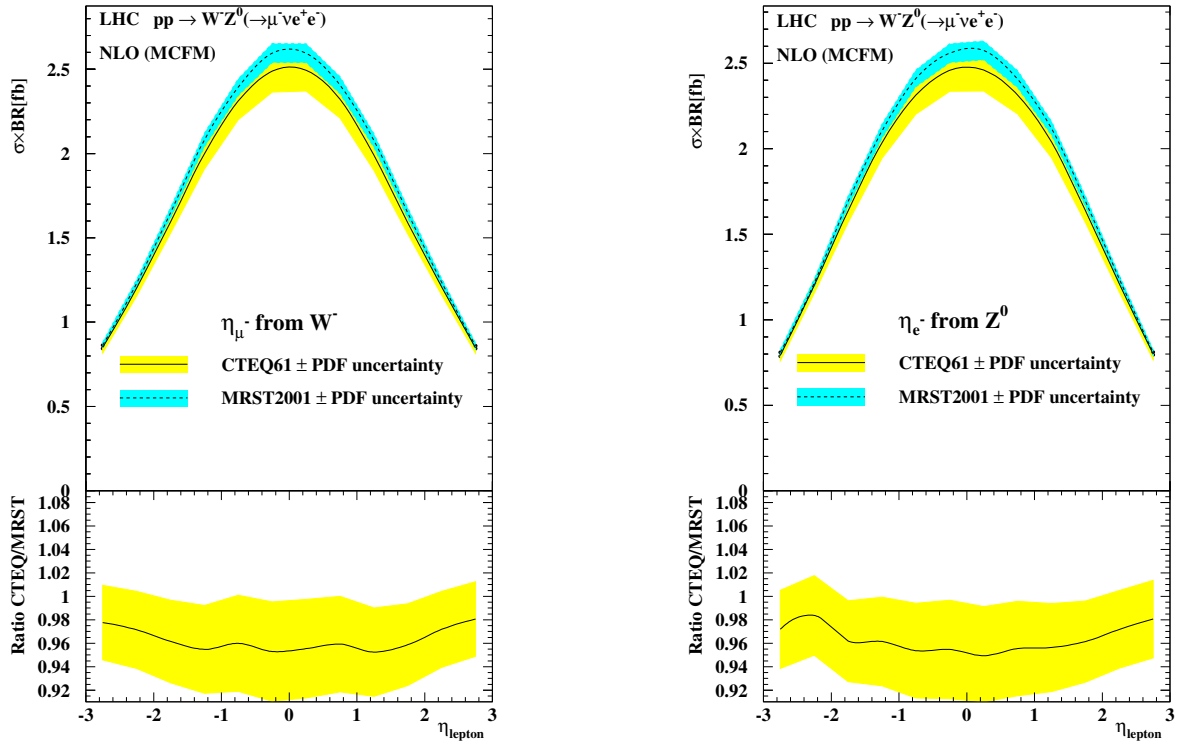


Fig. 22: Left: pseudo-rapidity distribution of the decay lepton of the W^- from inclusive $W^- Z^0$ production and right: pseudo-rapidity distribution of a decay lepton of the Z^0 .

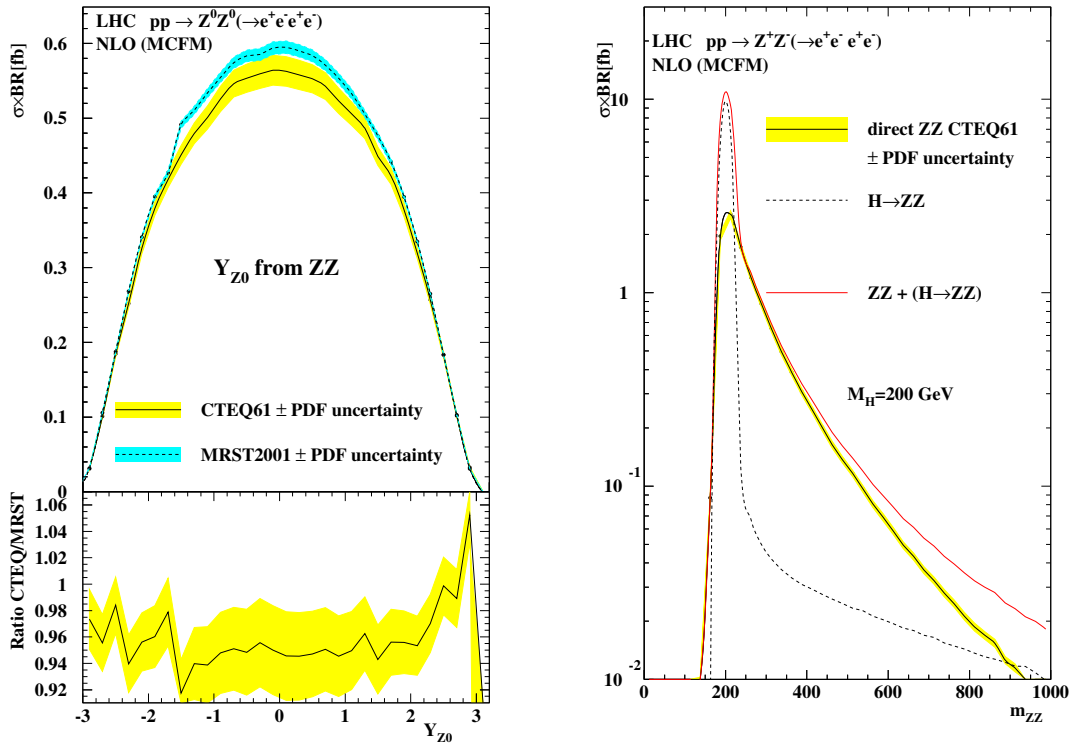


Fig. 23: Left: rapidity distribution of the leading Z from inclusive ZZ production and right: invariant mass of the ZZ pair for non-resonant continuum production compared to resonant pair production via the SM Higgs decay.

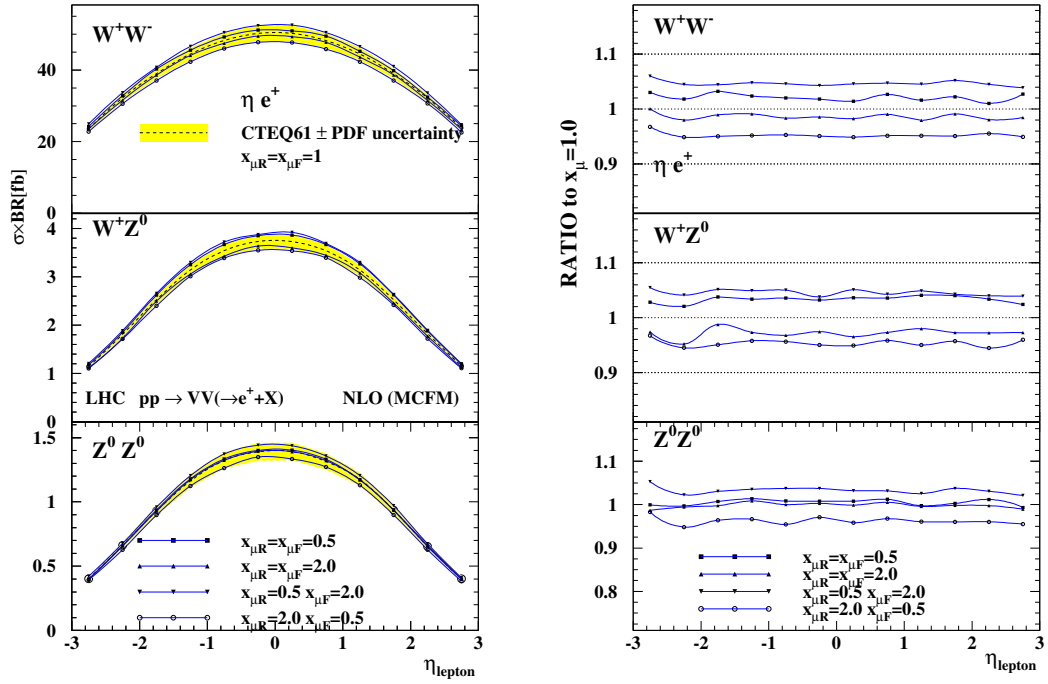


Fig. 24: Left: pseudo-rapidity distributions of leptons from various boson pair production processes and different scale settings and right: ratio of predictions relative to $x_{\mu} = 1$.

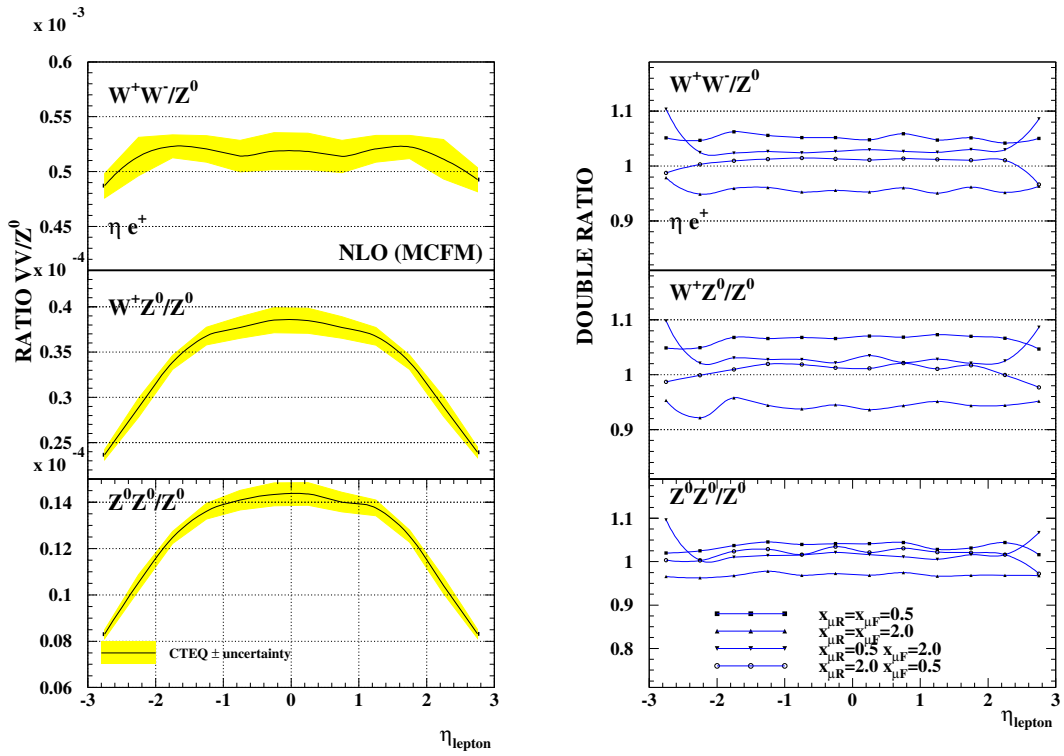


Fig. 25: Left: the ratio of pseudo-rapidity distributions of leptons from boson pair production processes normalised to single Z production and right: the double ratio VV/Z of predictions for different scales relative to $x_{\mu} = 1$.

Table 6: Total cross-sections and systematic uncertainties within the experimental acceptance for pair production processes.

| | WW | ZZ | W^+Z^0 | W^-Z^0 |
|--|------------|------------|------------|------------|
| CTEQ61 [fb] | 475.7 | 11.75 | 31.81 | 20.77 |
| $\Delta_{\text{PDF}}^{\text{CTEQ}}$ [fb] | ± 17.0 | ± 0.48 | ± 1.12 | ± 0.80 |
| $\Delta_{\text{PDF}}^{\text{CTEQ}}$ [%] | ± 3.6 | ± 4.1 | ± 3.5 | ± 3.8 |
| MRST [fb] | 494.2 | 12.34 | 32.55 | 21.62 |
| $\Delta_{\text{PDF}}^{\text{MRST}}$ [fb] | ± 6.3 | ± 0.19 | ± 0.49 | ± 0.41 |
| $\Delta_{\text{PDF}}^{\text{MRST}}$ [%] | ± 1.3 | ± 1.6 | ± 1.5 | ± 1.9 |
| Δ_{pert} [%] | +4.6 | +3.3 | +4.6 | +4.8 |
| | -4.9 | -3.8 | -4.7 | -4.7 |

can be measured at LHC, as well as to investigate their systematic uncertainties.

In the study presented here we have calculated both the differential (in rapidity) and inclusive cross sections for W, Z and high-mass Drell-Yan (Z/γ^*) production. Here "inclusive" refers to the results obtained by integrating the differential cross sections over a rapidity range similar to the experimentally accessible region, which might be more relevant than the complete cross section which also includes the large-rapidity tails.

Such a prediction would then be compared to the experimental measurements at LHC, which will allow for precise tests of the Standard Model as well as to put strong constraints on the parton distribution functions (PDFs) of the proton. It is clear that in the experiment only the rapidity and transverse momenta of the leptons from the vector boson decays will be accessible, over a finite range in phase space. In order to compute the rapidity of the vector boson by taking into account the finite experimental lepton acceptance, Monte Carlo simulations have to be employed which model vector boson production at the best possible precision in QCD, as for example the program MC@NLO [17]. The so computed acceptance corrections will include further systematic uncertainties, which are not discussed here.

1.5.1 Parameters and analysis method

The NNLO predictions have been implemented in the computer code VRAP [33], which has been modified in order to include ROOT [34] support for producing ntuples, histograms and plots. The code allows to specify the collision energy (14 TeV in our case), the exchanged vector boson (γ^* , Z, Z/γ^* , W^+ , W^-), the scale Q of the exchanged boson (M_Z , M_W or off-shell, e.g. $Q = 400$ GeV), the renormalization and factorization scales, the invariant mass of the di-lepton system (fixed or integrated over a specified range), the value of the electro-magnetic coupling ($\alpha_{\text{QED}} = 1/128$ or $\alpha_{\text{QED}}(Q)$) and the number of light fermions considered. Regarding the choice of pdfs, the user can select a pdf set from the MRST2001 fits [35] or from the ALEKHIN fits [36], consistent at NNLO with variable flavour scheme. We have chosen the MRST2001 NNLO fit, mode 1 with $\alpha_s(M_Z) = 0.1155$ [35], as reference set.

The program is run to compute the differential cross section $d\sigma/dY$, Y being the boson rapidity, at a fixed number of points in Y . This result is then parametrized using a spline interpolation, and the thus found function can be integrated over any desired rapidity range, such as $|Y| < 2$, $|Y| < 2.5$ or $|Y| < 3$, as well as over finite bins in rapidity. For the study of on-shell production the integration range over the di-lepton invariant mass M_{ll} was set to $M_V - 3\Gamma_V < M_{ll} < M_V + 3\Gamma_V$, with M_V and Γ_V the vector boson mass and width. This simulates an experimental selection over a finite signal range.

The systematic uncertainties have been divided into several categories: The PDF uncertainty is

estimated by taking the maximum deviation from the reference set when using different PDFs from within the MRST2001 set or the ALEKHIN set. The latter difference is found to give the maximal variation in all of the investigated cases. The renormalization and factorization scales $\mu = \mu_R, \mu_F$ have been varied between $0.5 < \mu/Q < 2$, both simultaneously as well as fixing one to $\mu = Q$ and varying the other. The maximum deviation from the reference setting $\mu = Q$ is taken as uncertainty. The observed difference when using either a fixed or a running electro-magnetic coupling constant is also studied as possible systematic uncertainty due to higher-order QED effects. Since it is below the one per-cent level, it is not discussed further. Finally, in the case of Z production it has been checked that neglecting photon exchange and interference contributions is justified in view of the much larger PDF and scale uncertainties.

1.5.2 Results for W and Z production

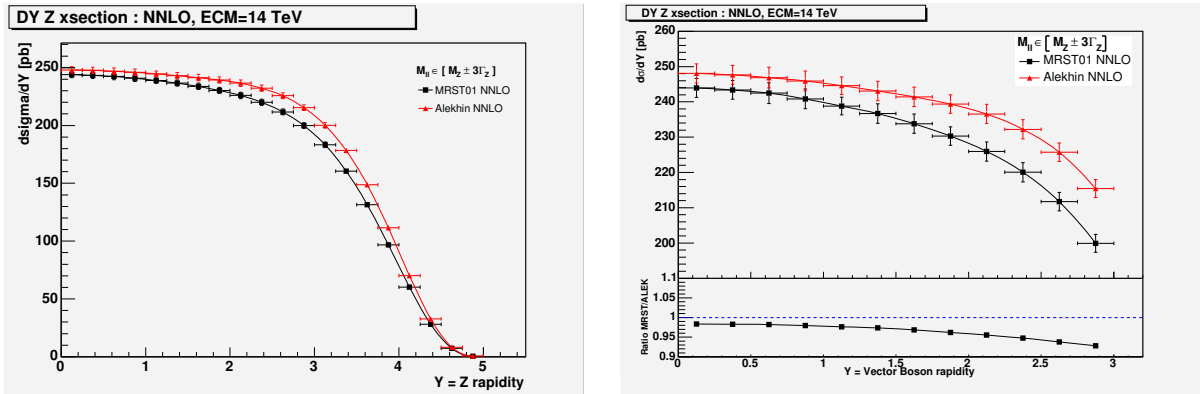


Fig. 26: Left : Drell-Yan Z production cross section (\times BR) at LHC energies, as a function of the Z rapidity, for two different PDF choices. Right : Zoom into a restricted rapidity region, with the ratio of the predictions for the two different PDF sets as lower inset. The error bars indicate the scale uncertainties.

In Fig. 26 the results for Z production at LHC are shown for two different choices of PDF set, as a function of the boson rapidity. It can be seen that the predictions differ by about 2% at central rapidity, and the difference increases to about 5% at large rapidity. A similar picture is obtained when integrating the differential cross section up to rapidities of 2, 2.5 and 3 (Table 7). The more of the high-rapidity tail is included, the larger the uncertainty due to the PDF choice. From Table 1 it can also be seen that the scale uncertainties are slightly below the one per-cent level. It is worth noting that the choice of the integration range over the di-lepton invariant mass can have a sizeable impact on the cross section. For example, increasing the range from the standard value to $66 \text{ GeV} < M_Z < 116 \text{ GeV}$ increases the cross section by 8%.

Table 7: NNLO QCD results for W and Z production at the LHC for the integration over different rapidity ranges. Also given are the relative uncertainties due to the choice of the PDFs and of the renormalization and factorization scale. The numbers include the branching ratio $Z(W) \rightarrow ee(e\nu)$.

| Channel range | Z prod. | | | W prod. | | |
|--------------------|-----------|-------------|-----------|-----------|-------------|-----------|
| | $ Y < 2$ | $ Y < 2.5$ | $ Y < 3$ | $ Y < 2$ | $ Y < 2.5$ | $ Y < 3$ |
| cross section [nb] | 0.955 | 1.178 | 1.384 | 9.388 | 11.648 | 13.800 |
| Δ PDF [%] | 2.44 | 2.95 | 3.57 | 5.13 | 5.47 | 5.90 |
| Δ scale [%] | 0.85 | 0.87 | 0.90 | 0.99 | 1.02 | 1.05 |

The results for W production (Table 7) have been obtained by first calculating separately the cross sections for W^+ and W^- production, and then adding these up. Again we observe an increase of the PDF uncertainty when going to larger rapidity ranges. Compared to the Z production, here the PDF uncertainties are larger, between 5 and 6%, whereas the scale uncertainties are of the same level, $\approx 1\%$. It is interesting to note that the PDF uncertainty for W^- production is about 10 - 20% (relative) lower than that for W^+ .

A considerable reduction in systematic uncertainty can be obtained by calculating cross section ratios. Two options have been investigated, namely the ratios $\sigma(W^+)/\sigma(W^-)$ and $\sigma(W)/\sigma(Z)$. As can be seen from Figure 27, the PDF uncertainties are reduced to the 0.7% level in the former ratio, and to about 2% in the latter. The scale uncertainties are reduced to the 0.15% level in both cases. Taking such ratios has also the potential advantage of reduced experimental systematic uncertainties, such as those related to the acceptance corrections.

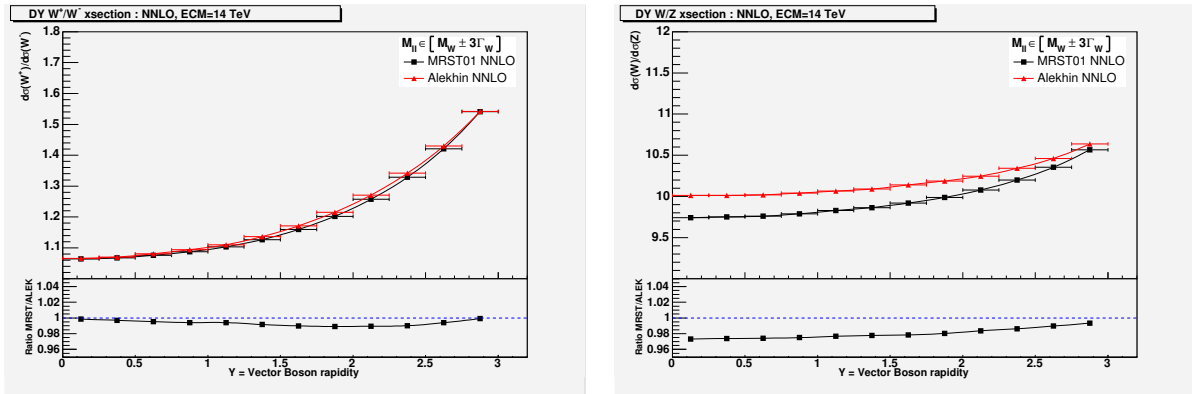


Fig. 27: Ratio of the production cross sections for W^+ , W^- (left), and W, Z (right), as a function of rapidity, for two different PDF sets. The inserts show the ratios of the results for the two PDF choices.

1.5.3 Results for high-mass Drell-Yan processes

Similarly to on-shell W and Z production we have also analyzed the high-mass Drell-Yan process, namely Z/γ^* production at a scale of $Q = 400$ GeV. In this case the di-lepton invariant mass has been integrated over the range $M_{ll} = 400 \pm 50$ GeV. Here the PDF uncertainties are found between 3.7% and 5.1% for the various integration ranges over rapidity, somewhat larger than for on-shell production. However, by normalizing the high-mass production cross section to the on-shell case, the PDF uncertainties are considerably reduced, being 1.2 - 1.5%.

The systematic uncertainties related to the renormalization and factorization scale are reduced (Δ scale $\approx 0.2\%$) when going to the high-mass exchange, as expected from perturbative QCD with a decreasing strong coupling constant. In this case a normalization of the cross section to the on-shell case does not give an improvement. However, since the scale uncertainties are well below the PDF uncertainties, this is less of an issue for the moment.

1.5.4 Summary

We have studied NNLO QCD predictions for W and Z production at LHC energies. We have identified the choice of PDF set as the dominant systematic uncertainty, being between 3 and 6%. The choice of the renormalization and factorization scale leads to much smaller uncertainties, at or below the 1% level. In particular we have shown that the systematic uncertainties can be sizeably reduced by taking ratios of cross sections, such as $\sigma(W^+)/\sigma(W^-)$, $\sigma(W)/\sigma(Z)$ or $\sigma(Z/\gamma^*, Q = 400 \text{ GeV})/\sigma(Z/\gamma^*, Q = M_Z)$. For such ratios it can be expected that also part of the experimental uncertainties cancel. With theoretical

uncertainties from QCD at the few per-cent level the production of W and Z bosons will most likely be the best-known cross section at LHC.

Concerning the next steps, it should be considered that at this level of precision it might become relevant to include also higher-order electro-weak corrections. In addition, since experimentally the boson rapidity will be reconstructed from the measured lepton momenta, a detailed study is needed to evaluate the precision at which the acceptance correction factors for the leptons from the boson decays can be obtained. For this Monte Carlo programs such as MC@NLO should be employed, which combine next-to-leading-order matrix elements with parton showers and correctly take account of spin correlations.

References

- [1] Dittmar, M. and Pauss, F. and Zurcher, D., Phys. Rev. **D56**, 7284 (1997).
- [2] Acosta, D. et al., Phys. Rev. Lett. **94**, 091803 (2005).
- [3] Bellavance, A. M., *W/z production cross sections and asymmetries at e(cm) = 2-tev*. Preprint hep-ex/0506025, 2005.
- [4] Abazov, V. M. et al., Phys. Rev. Lett. **95**, 051802 (2005).
- [5] Taffard, A., *Top production cross section from cdf*. To appear in the proceedings of 32nd International Conference on High-Energy Physics (ICHEP 04), Beijing, China, 16-22 Aug 2004.
- [6] Bortoletto, D., *Searching for susy at the tevatron*. Preprint hep-ex/0412013, 2004.
- [7] Heister, A. et al., Eur. Phys. J. **C38**, 147 (2004).
- [8] Abbiendi, G. et al., Phys. Lett. **B609**, 212 (2005).
- [9] Heister, A. et al., Eur. Phys. J. **C28**, 1 (2003).
- [10] Abdallah, J. et al., Eur. Phys. J. **C37**, 405 (2004).
- [11] Chekanov, S. et al., Phys. Rev. **D67**, 012007 (2003).
- [12] Giele, W. and Whalley, M. R., *Lhapdf v3: Les houches accord pdf*. Available on <http://durpdg.dur.ac.uk/lhapdf/>.
- [13] Pumplin, J. et al., JHEP **07**, 012 (2002).
- [14] Martin, A. D. et al., Eur. Phys. J **C23**, 73 (2002).
- [15] G. Laštovička-Medin et al., *Precision limits for hera dis cross section measurement*. These proceedings.
- [16] Corcella, G. et al., JHEP **01**, 010 (2001).
- [17] Frixione, S. and Webber, B. R., JHEP **06**, 029 (2002).
- [18] Stirling, W. J., private communication.
- [19] Barlow, R., ECONF **C030908**, WEMT002 (2003).
- [20] Altarelli, G. and Parisi, G., Nucl.Phys. **B126**, 298 (1977).
- [21] Gribov, V.N. and Lipatov, L.N., Sov.J.Nucl.Phys **15**, 438 (1972).
- [22] Lipatov, L. N., Sov.J.Nucl.Phys **20**, 94 (1975).
- [23] Dokshitzer, Yu. L., JETP **46**, 641 (1977).
- [24] Lipatov, L. N., Sov. J. Nucl. Phys. **23**, 338 (1976).
- [25] Kuraev, E. A. and Lipatov, L. N. and Fadin, Victor S., Sov. Phys. JETP **45**, 199 (1977).
- [26] Balitsky, I. I. and Lipatov, L. N., Sov. J. Nucl. Phys. **28**, 822 (1978).
- [27] Devenish, R. C. E. and Cooper-Sarkar, A. M., *Deep Inelastic Scattering*. Oxford University Press, Oxford, 2004.
- [28] Campbell, J. M. and Ellis, R. K., *Mcfm v4.0: A monte carlo for femtobarn processes at hadron colliders*. Available on <http://mcfm.fnal.gov/>.

- [29] Stump, D. et al., JHEP **10**, 046 (2003).
- [30] Martin, A. D. and Roberts, R. G. and Stirling, W. J. and Thorne, R. S., Eur. Phys. J. **C28**, 455 (2003).
- [31] Jones, R. W. L. and Ford, M. and Salam, G. P. and Stenzel, Hasko and Wicke, Daniel, JHEP **12**, 007 (2003).
- [32] Anastasiou, C. and Dixon, L. J. and Melnikov, K. and Petriello, F., Phys. Rev. **D69**, 094008 (2004).
- [33] Dixon, L., private communication.
- [34] Brun, R. and Rademakers, F., Nucl. Instrum. Meth. **A389**, 81 (1997).
- [35] Martin, A. D. and Roberts, R. G. and Stirling, W. J. and Thorne, R. S., Phys. Lett. **B531**, 216 (2002).
- [36] Alekhin, S., Phys. Rev. **D68**, 014002 (2003).